



## Simplified model of a two-layer aquifer system under stress of geogenic groundwater salinization

### D3.1 – Konzeptionelles Modell

Main Authors:

Dwight Baldwin, Christoph Sprenger

Date: 05/03/2024

## Technical References

Project Acronym	GeoSalz
Project Title	Dynamik des Salzwasseraufstiegs zur Früherkennung gefährdeter Brunnen und Quantifizierung des hydraulischen Entlastungspotentials - Dynamics of saltwater flow for early detection of threatened wells and quantification of the hydraulic discharge potential
Project ID N°:	
Topic:	Geogene Grundwasserversalzung
Type of funding	Sponsoring
Project Coordinator	Dr. Christoph Sprenger
Project Duration	3.5 years (0.5 years extended)

Deliverable No.	3.1
Dissemination level <sup>1</sup>	PU
Work Package	3
Task	3
Lead beneficiary	BWB
Contributing beneficiary(ies)	KWB
Due date of deliverable	February 2024
Actual submission date	February 2024

<sup>1</sup> PU = Public

PP = Restricted to other programme participants (including the Commission Services)

RE = Restricted to a group specified by the consortium (including the Commission Services)

CO = Confidential, only for members of the consortium (including the Commission Services)

## Document history

V	Date	Beneficiary	Author
2.0	January 2024	BWB	Baldwin, Sprenger
2.3	February 2024	BWB	Quality Assurance: Gunnar Lorenzen
3	March 2024	BWB	Baldwin, Sprenger

## Disclaimer

*We have made every attempt to ensure that the information contained in this report has been obtained to the best of our knowledge and belief. However, KWB is not responsible for any errors or omissions, or for the results obtained from the use of this information. All information in this site is provided "as is", with no guarantee of completeness, accuracy, timeliness or of the results obtained from the use of this information*

## Table of Contents

TECHNICAL REFERENCES.....	2
DOCUMENT HISTORY.....	3
SUMMARY.....	8
ZUSAMMENFASSUNG.....	10
1. INTRODUCTION .....	13
2. STUDY AREA.....	13
3. MODEL DESCRIPTION .....	14
3.1. HYDRAULIC CONDUCTIVITY.....	17
3.2. WELL DESIGN AND ABSTRACTION RATES .....	17
3.3. CONSTANT HEAD .....	17
3.4. RIVER PACKAGE.....	18
3.5. GROUNDWATER RECHARGE .....	19
3.6. GENERAL HEAD .....	19
3.7. MODEL DISCRETIZATION AND TRANSPORT PROPERTIES .....	20
3.8. SCENARIO DESCRIPTION .....	20
4. RESULTS .....	22
4.1. NON-PUMPING MODEL .....	22
4.2. BASE MODEL .....	25
4.3. SCENARIO GROUP 1 .....	30
4.4. SCENARIO GROUP 2 .....	31
4.5. SCENARIO GROUP 3 .....	32
4.6. SCENARIO GROUP 4 .....	33
4.7. SCENARIO GROUP 5 .....	34
5. CONCLUSIONS.....	35
REFERENCES.....	36
ANNEX 1: SUPPLEMENTARY INFORMATION .....	38
ANNEX 2: SUPPLEMENTARY RESULTS FOR MODEL SCENARIOS .....	44

## TABLE OF TABLES

Table 1: Model Parameters .....	16
Table 2: Model Scenarios overview .....	21
Table 3: Water balance for non-pumping scenario.....	23
Table 4: Water balance base model.....	28
Table 5: Density corrections for observed hydraulic heads during Geosalz field sampling .....	38
Table 6: Chlorid Analysen vom BWB Hydrochemie ab 2020 Langer See .....	42
Table 7: Well field K profiles 1983 .....	43

## TABLE OF FIGURES

Figure 1: Schematic overview conceptual model.....	15
Figure 2: Simulated chloride concentration cross-sections at T = 0, 500, 1000, 1500 and 2000 years (red dots = observation cells; blue line = river cells; brown layer = Holstein aquitard cells) .....	22
Figure 3: Cross sections of hydraulic heads non-pumping scenario .....	24
Figure 4: Simulated chloride concentration cross-sections at T = 0, 1, 10, 20 and 40 years of pumping (red dots = observation/abstraction well cells; blue line = river cells; brown layer = Holstein aquitard cells).....	26
Figure 5: Breakthrough curves concentration vs. time (left); cumulated load of chloride vs. time (right).....	27
Figure 6: Cross sections of hydraulic heads for base scenario .....	29
Figure 7: Comparison SEAWAT with MT3D solution .....	29
Figure 8: Mean annual load (t/a) and chloride concentration (mg/l) over 40a of pumping for scenario group 1 .....	30
Figure 9: Mean annual chloride load (t/a) and chloride concentration (mg/l) over 40a of pumping for scenario group 2 .....	31
Figure 10: Mean annual chloride (t/a) and chloride concentration (mg/l) over 40a of pumping for scenario group 3.....	32
Figure 11: Mean annual chloride load (t/a) and chloride concentration (mg/l) over 40a of pumping for scenario group 4 .....	33
Figure 12: Mean annual chloride load (t/a) and chloride concentration (mg/l) over 40a of pumping for scenario group 5 .....	34
Figure 13: Well profile –K-well field 1983.....	40
Figure 14: Observed chloride concentration in K-well field vs well ID from 1983 to 1995 (BWB data) .....	40

Figure 15: Observed chloride concentration in K-well field vs well ID from 2008 to 2021 (BWB data)	41
Figure 16: Observed chloride concentration in K-well field vs year from 1983 to 1995 (BWB data)	41
Figure 17: Observed chloride concentration in K-well field vs year from 2008 to 2021 (BWB data)	41
Figure 18: Observed chloride concentration in K-well field vs year per abstraction (BWB data)..	41
Figure 19: Profilschnitt K-Galerie Nord- Süd von Asbrand-Ing	43
Figure 20: Profilschnitt K-galerie Ost-West von Asbrand-Ing	43
Figure 21: Cross sections, breakthrough curve, and water budget for scenario S1.1; $Q_2 = 0 \text{ m}^3\text{d}^{-1}$	45
Figure 22: Cross sections, breakthrough curve, and water budget for scenario S1.2; $Q_2 = 100 \text{ m}^3\text{d}^{-1}$	46
Figure 23: Cross sections, breakthrough curve, and water budget for scenario S1.3; $Q_2 = 200 \text{ m}^3\text{d}^{-1}$	47
Figure 24: Cross sections, breakthrough curve, and water budget for scenario S1.4; $Q_2=300 \text{ m}^3\text{d}^{-1}$	48
Figure 25: Cross sections, breakthrough curve, and water budget for scenario S1.6; $Q_2=400 \text{ m}^3\text{d}^{-1}$	49
Figure 26: Cross sections, breakthrough curve, and water budget for scenario S2.1; $Q_{\text{TOT}} = 300 \text{ m}^3\text{d}^{-1}$	50
Figure 27: Cross sections, breakthrough curve, and water budget for scenario S2.2; $Q_{\text{TOT}} = 400 \text{ m}^3\text{d}^{-1}$	51
Figure 28: Cross sections, breakthrough curve, and water budget for scenario S2.3; $Q_{\text{TOT}} = 600 \text{ m}^3\text{d}^{-1}$	52
Figure 29: Cross sections, breakthrough curve, and water budget for scenario S2.5; $Q_{\text{TOT}} = 1800 \text{ m}^3\text{d}^{-1}$	53
Figure 30: Cross sections, breakthrough curve, and water budget for scenario S2.6; $Q_{\text{TOT}} = 2400 \text{ m}^3\text{d}^{-1}$	54
Figure 31: Cross sections, breakthrough curve, and water budget for scenario S3.1	55
Figure 32: Cross sections, breakthrough curve, and water budget for scenario S3.3	56
Figure 33: Cross sections, breakthrough curve, and water budget for scenario S3.4	57
Figure 34: Cross sections, breakthrough curve, and water budget for scenario S3.5	58
Figure 35: Cross sections, breakthrough curve, and water budget for scenario S4.1	59
Figure 36: Cross sections, breakthrough curve, and water budget for scenario S4.2	60
Figure 37: Cross sections, breakthrough curve, and water budget for scenario S4.4	61

Figure 38: Cross sections, breakthrough curve, and water budget for scenario S4.5 .....	62
Figure 39: Cross sections, breakthrough curve, and water budget for scenario S5.1 .....	63
Figure 40: Cross sections, breakthrough curve, and water budget for scenario S5.2 .....	64
Figure 41: Cross sections, breakthrough curve, and water budget for scenario S5.4 .....	65
Figure 42: Cross sections, breakthrough curve, and water budget for scenario S5.5 .....	66

## Summary

In this study, recommendations for the control of geogenic groundwater salinization for drinking water supply are developed based on a simplified numerical flow and mass transport model for a bank filtration gallery at the Berlin-Friedrichshagen waterworks. The aim of the model is to better understand the influence of operational practice (e.g. well control) and the hydrogeological boundary conditions (e.g. river level) on saltwater migration in order to ensure safe groundwater extraction at sites at risk of salinization. Based on scenario simulations, recommendations are derived to protect drinking water wells from qualitative impairment while maximizing the use of bank filtration under the stress of geogenic groundwater salinization.

The boundary conditions and parameters of the model are largely based on measured variables in the study area or are based on well-founded assumptions. However, the model represents an idealized approximation of groundwater flow and salt transport and simulates the trends observed in the wells. Transfer to other well locations is therefore only possible to a limited extent.

Flow and transport simulations were calculated with the three-dimensional finite difference groundwater model MODFLOW-2005 and MT3DMS. Density-dependent model simulations were calculated with SEAWAT. However, due to the relatively small density differences used in the model, no significant influence of density-dependent flow could be determined.

The base model is intended to reproduce the measured chloride concentrations after the K-Gallery was commissioned in 1984. The simulation period was set at 40 years under constant conditions. This period is longer than the effective operating period from the start of commissioning until the new construction of the wells in 2022/23. One challenge in developing the model was that the simulated chloride concentrations are largely determined by the starting conditions. However, measurements of the spatial distribution of the study area before the start of groundwater extraction are hardly known. It is therefore not possible to determine the spatial distribution of the chloride concentrations as starting conditions. Therefore, the base model without well extraction (representing quasi-natural conditions) was used to calculate a spatial distribution of the chloride concentration. After 2000 simulated years, a quasi-equilibrium state was reached. The simulations in the non-pumping model clearly show that the transport processes in the deep geological subsurface require periods of thousands of years to reach a quasi-equilibrium state. In contrast to the model, the boundary conditions in nature are not stable over such long periods of time, and the current state must be regarded as dynamic. Based on the simulated chloride concentration from the non-pumping scenario, the time step  $T = 2000a$  was used as the starting condition for pumping scenarios. The simulated chloride values in the base model correspond to the measured trends of the hydrochemical development of the K-Gallery due to i) the maximum chloride values of approx. 450 mg/l, ii) the rapid increase at the beginning of commissioning and after several years of operation and iii) the slight but steady increase in Cl values over many years. This showed that the basic model is capable of simulating the hydrochemical developments observed in the wells. A model-based explanation for the hydrochemical development of the past could thus be developed for the first time.

Scenario 1 examines the function of the central well as a defense well. The purpose of a defense well is to intercept pollutants from the groundwater in order to prevent them from entering the wells of neighboring wells and spreading further in the aquifer. However, it is questionable

whether an increase in well abstraction directly above a window in the groundwater inhibitor (Holstein window) can lead to a disproportionate increase in the salt load and thus to increased mobilization of the salt. Based on the scenarios, it can be concluded that the central well protects the neighboring wells from salt intrusion but the annual salt load increases by approximately 10 tons. However, the simulations did not show an excessive increase in salt loads under the given conditions. The function of the central well as a defense well to prevent the spread of saline groundwater in the upper aquifer was confirmed by the simulations. The current practice of operating the central well with a lower pumping capacity compared to the neighboring wells proved to be effective.

In Scenario 2, the total extraction volume of the wells was gradually increased. As expected, an increase in well abstraction leads to increased mobilization of the deep groundwater and thus to increased salinity in the wells. In this scenario, it should be investigated how the increase in total abstraction affects the amount of bank filtrate, which leads to an equalization of the salt input into the wells. Scenario 2 shows that, under the given boundary conditions, the central well retains its protective function for the neighboring wells and the upper aquifer even if the withdrawal volume increases.

The question in scenario 3 was to what extent the natural heterogeneities of hydraulic conductivity in the lower aquifer can influence saltwater migration. It was shown that the natural heterogeneities can lead to a sharp increase in salt concentration and load. In the central well, chloride concentrations were simulated that are far above the drinking water limit and would pose considerable difficulties for the operation of the well gallery. A hydrogeological investigation of the underlying subsoil is recommended, especially in places where groundwater-inhibiting layers are missing.

In scenario 4, groundwater recharge was varied between 50 and 150 mm/year. It was shown that the change in groundwater recharge has no significant influence on the simulated concentrations and loads. Compared to other studies, the influence of groundwater recharge is slightly underestimated in the model, but is consistent with the large-scale numerical model and is within a plausible range. The K-Gallery is a special case in this respect, as the wells receive bank filtrate from two sides (Langer See and Große Krampe) and are hardly influenced by direct groundwater recharge.

In scenario 5, the extent to which the river level influences salt migration was investigated. It is obvious that an increase in the water level causes greater hydraulic gradients between surface water and groundwater and leads to higher bank filtrate proportions and thus to a lower saltwater influence. The simulations in this scenario show that even small changes in the water level of a few cm in the Dahme lead to relatively large changes in the chloride concentration and loads in the wells. In the event of a prolonged drop below current water levels, greatly increased chloride levels in the wells must therefore be expected.

## Zusammenfassung

In dieser Studie werden Empfehlungen zur Kontrolle einer geogenen Grundwasserversalzung für die Trinkwasserversorgung auf der Grundlage eines vereinfachten numerischen Strömungs- und Stofftransportmodells für eine Uferfiltrationsgalerie im Wasserwerk Berlin-Friedrichshagen entwickelt. Ziel des Modells ist es, den Einfluss der betrieblichen Praxis (z.B. Brunnensteuerung) und den hydrogeologischen Randbedingungen (z.B. Flusspegel) auf die Salzwassermigration besser zu verstehen um eine sichere Grundwasserförderung an versalzungsgefährdeten Standorten gewährleisten zu können. Auf der Grundlage von Szenariosimulationen werden Empfehlungen abgeleitet, um Trinkwasserbrunnen vor qualitativen Beeinträchtigungen zu schützen und gleichzeitig die Nutzung der Uferfiltration unter dem Stress der geogenen Grundwasserversalzung zu maximieren.

Die Randbedingungen und Parameter des Modells basieren weitgehend auf gemessenen Größen im Untersuchungsgebiet oder beruhen auf begründeten Annahmen. Das Modell stellt jedoch eine idealisierte Annäherung der Grundwasserströmung und des Salztransports dar und simuliert die beobachteten Trends in den Brunnen. Eine Übertragung auf andere Brunnenstandorte ist daher nur bedingt möglich.

Strömungs- und Transportsimulationen wurden mit dem dreidimensionalen Finite-Differenzen-Grundwassermodell MODFLOW-2005 und MT3DMS gerechnet. Dichte-abhängige Modellsimulationen wurden mit SEAWAT gerechnet. Aufgrund der im Modell genutzten relativ geringen Dichteunterscheide, konnte jedoch kein signifikanter Einfluss der dichte-abhängigen Strömung festgestellt werden.

Das Basismodell soll die gemessenen Chlorid Konzentrationen nach Inbetriebnahme der K-Galerie im Jahr 1984 wiedergeben. Der Simulationszeitraum wurde auf 40 Jahre bei konstanten Bedingungen festgelegt. Dieser Zeitraum ist länger als die effektive Betriebsdauer vom Beginn der Inbetriebnahme bis zum Neubau der Brunnen in den Jahren 2022/23. Eine Herausforderung bei der Modellentwicklung bestand darin, dass die simulierten Chlorid Konzentrationen wesentlich von den Startbedingungen bestimmt werden. Messungen der räumlichen Verteilung Untersuchungsgebiet vor dem Beginn der Grundwasserentnahme sind jedoch kaum bekannt. Es ist daher nicht möglich, die räumliche Verteilung der Chlorid Konzentrationen als Startbedingungen festzulegen. Daher wurde das Basismodell ohne Brunnen welches die quasi-natürliche Bedingungen darstellt genutzt, um eine räumliche Verteilung der Chlorid Konzentration zu berechnen. Nach 2000 simulierten Jahren wurde ein Quasi-Gleichgewichtszustand erreicht. Die Simulationen im Nicht-Pumpen Modell machen deutlich dass die Transportprozesse im tiefen geologischen Untergrund Zeiträume von tausenden Jahren benötigen, um einen quasi-Gleichgewichtszustand zu erreichen. Im Gegensatz zum Modell, sind die Randbedingungen in der Natur über solche lange Zeiträume nicht stabil, und der aktuelle Zustand muss als ein dynamischer betrachtet werden. Ausgehend von der simulierten Chloridkonzentration aus dem Nicht-Pump-Szenario wurde der Zeitschritt  $T = 2000a$  als Startbedingung für Pump-Szenarien verwendet. Die simulierten Chloridwerte im Basismodell entsprechen den gemessenen Trends der hydrochemischen Entwicklung der K-Galerie durch i) die Chlorid Höchstwerte von ca. 450 mg/l, ii) dem raschen Anstieg am Beginn der Inbetriebnahme und nach einigen Betriebsjahren Jahren Abfall und iii) dem langjährigen leichtem aber stetigen Anstieg der Cl-Werte. Damit konnte gezeigt werden, dass das Basismodell in der Lage ist, die in

den Brunnen beobachteten hydrochemischen Entwicklungen zu simulieren. Es konnte somit erstmals eine modellbasierte Erklärung für die hydrochemische Entwicklung der Vergangenheit entwickelt werden.

Im Szenario 1 wird die Funktion des zentralen Brunnens als Abwehrbrunnen untersucht. Ein Abwehrbrunnen soll Schadstoffe aus dem Grundwasser abfangen, um zu verhindern, dass diese in die Fassungen der Nachbarbrunnen gelangen und sich im Grundwasserleiter weiter ausbreiten. Es ist jedoch fraglich, ob eine Erhöhung der Brunnenentnahme direkt oberhalb eines Fensters im Grundwasserhemmer (Holsteinfenster) zu einer überproportionalen Erhöhung der Salzfracht und damit zu einer verstärkten Mobilisierung des Salzes führen kann. Anhand der Szenarien kann gefolgert werden, dass der zentrale Brunnen die benachbarten Brunnen vor dem Eindringen von Salz schützt. Die Simulationen zeigen, dass die Erhöhung der Pumpleistung des zentralen Brunnens oberhalb des Holstein-Fensters die mittlere jährliche Chloridfracht um ~10 Tonnen erhöht, ohne die Gesamtentnahme zu erhöhen. Unter den gegebenen Bedingungen zeigten die Simulationen jedoch keinen übermäßigen Anstieg der Salzfrachten. Die Funktion des zentralen Brunnens als Abwehrbrunnen zur Verhinderung der Ausbreitung von salzhaltigem Grundwasser im oberen Grundwasserleiter, konnte durch die Simulationen bestätigt werden. Die derzeitige Praxis, den Betrieb des Zentralbrunnens mit einer im Vergleich zu den Nachbarbrunnen geringeren Pumpleistung Brunnen zu betreiben, erwies sich als effektiv.

Im Szenario 2 wurde die Gesamtentnahmemenge der Brunnen schrittweise erhöht. Erwartungsgemäß führt eine Erhöhung der Brunnenentnahmen zu einer verstärkten Mobilisierung des Tiefengrundwassers und damit zu einem erhöhten Salzgehalt in den Brunnen führt. In diesem Szenario sollte untersucht werden, wie sich die Erhöhung der Gesamtentnahme auf die Menge des Uferfiltrats auswirkt, das zu einem Ausgleich des Salzeintrags in die Brunnen führt. Szenario 2 zeigt, dass unter den gegebenen Randbedingungen der zentrale Brunnen auch bei steigenden Entnahmemenge seine Schutzfunktion für die Nachbarbrunnen und dem oberen Grundwasserleiter behält.

Die Fragestellung im Szenario 3 war, inwieweit die natürlichen Heterogenitäten der hydraulischen Leitfähigkeit im unteren Grundwasserleiter die Salzwassermigration beeinflussen können. Es konnte gezeigt werden, dass die natürlichen Heterogenitäten zu einem starken Anstieg der Salzkonzentration und -fracht führen können. Im zentralen Brunnen wurden Chlorid Konzentrationen simuliert die weit über Trinkwassergrenzwert liegen und einen Betrieb der Brunnengalerie vor erhebliche Schwierigkeiten stellen würde. Besonders an Stellen an denen grundwasserhemmende Schichten fehlen, ist eine hydrogeologische Erkundung des liegenden Untergrunds zu empfehlen.

Im Szenario 4 wurde die Grundwasserneubildung zwischen 50 und 150 mm/a variiert. Es konnte gezeigt werden, dass die Veränderung der Grundwasserneubildung keinen signifikanten Einfluss auf die simulierten Konzentrationen und Frachten hat. Im Vergleich zu anderen Studien wird der Einfluss der Grundwasserneubildung im Modell etwas unterschätzt, steht aber im Einklang mit dem großskaligen numerischen Modell und liegt in einem plausiblen Bereich. Die K-Galerie ist in dieser Hinsicht ein Sonderfall, da die Brunnen von zwei Seiten (Langer See und Große Krampe) Uferfiltrat erhalten und kaum von direkter Grundwasserneubildung beeinflusst sind.

Im Szenario 5 wurde untersucht inwieweit der Flusspegel die Salzmigration beeinflusst. Es liegt auf der Hand, dass ein Anstieg des Wasserstands größere hydraulische Gradienten zwischen

Oberflächen- und Grundwasser bewirkt und zu höheren Uferfiltratanteilen und damit zu einem geringeren Salzwassereinfluss führt. Die Simulationen in diesem Szenario zeigen, dass bereits geringe Veränderungen des Wasserstands von wenigen cm in der Dahme zu relativ großen Änderungen der Chloridkonzentration und -frachten in den Brunnen führen. Im Falle einer längeren Unterschreitung der heutigen Wasserstände muss daher mit stark erhöhten Chloridwerten in den Brunnen gerechnet werden.

## 1. Introduction

In many coastal and inland areas around the world, migration of saline water into a fresh water aquifer is a common problem (van Weert et al., 2009). Due to the increasing pumping of groundwater, geogenic salinization in drinking water aquifers in northern Germany and also Berlin has increasingly come into focus since the beginning of the 20th century at the latest (Grube and Martens, 2011; Grube et al., 2000; Schramm and Herd, 2020).

Elevated chloride concentrations have been detected at individual wells at five of the nine BWB waterworks and historical research show that salinization phenomena occurred at some sites before groundwater was first used for drinking water more than 100 years ago (Schramm and Herd, 2020). The upwelling of salty water along the hydraulic discharge areas is in some cases natural. The dynamics of this geogenic salt intrusion however is not fully understood, and therefore poses a threat to Berlin's water supply sustainability.

In this study, recommendations are made to control geogenic saltwater intrusion into an inland aquifer for drinking water supply based on a simplified numerical flow and solute transport model of a riverbank filtration well gallery at the waterworks Berlin-Friedrichshagen. The model aims to better understand the risks levels associated with operational practices (e.g. pumping schemes) and hydrogeological boundary conditions (e.g. river stages). Based on scenario simulations, recommendations are formulated to protect drinking water wells from qualitative impairments while maximizing use of riverbank filtration sites under stress of geogenic groundwater salinization.

## 2. Study area

The project study area comprises the K-gallery of the Berlin-Friedrichshagen waterworks, where there is evidence of elevated chloride in individual production wells. The filter screens of the K-gallery wells are above the underlying Holstein aquitard. In the case of the GeoSalz study area, a gap in the Holstein aquitard is a likely explanation for the observed salinization at the K gallery wells.

Observation wells and production wells in the study area exist within 3 hydrogeological units (see annex 1 cross section Figure 19 and Figure 20). The top unit represents the shallow aquifer, consisting primarily of medium grain sand and pockets of coarse sand, and is fed mostly by riverbank filtrate and local groundwater recharge. This aquifer represents the Weichsel and Saale glacial and interglacial deposits (Limberg and Thierbach, 2002). The second unit contains medium to fine sand, with intercalated layers of marl, clay and glacial till. This aquitard (see chapter 3.1) contains the material that makes up the hydraulically-important Holstein layer, which inhibits vertical groundwater flow. However, there are discontinuities within this layer made of medium sand, and vertical water and salt interflow is evident in sample wells. The lower unit is the aquifer 3 representing the region below the Holstein and consists of quaternary medium to fine sands. This aquifer represents the Elster glacial and interglacial deposits (Limberg and Thierbach, 2002). The underlying units are assigned to the Tertiary. In the BWB classification, these layers are assigned to aquifer 3, in contrast to Limberg and Thierbach (2002) who classifies a fourth aquifer.

Salt concentrations in this region are the highest (2100-4000 mg/l). Hydrochemical data at the K-gallery of the Friedrichshagen waterworks corroborates the existence of brackish and brackish-salt water in the area. Deeper wells are often more likely to be brackish (Cl > 300 mg/l) or brackish-salt (Cl > 1000 mg/l) while shallow wells are more likely to be fresh.

### **3. Model description**

The model presents an idealized approximation of groundwater flow and transport of salt, approximated through chloride, around the observed discontinuity in the Holstein aquitard. The model is adapted from a model created by Tobias Felsch during his master thesis (Felsch, 2022). Additions and modifications are done to the Felsch conceptual model, including but not limited to revising boundary conditions, improving the model grid resolution, increasing the depth of the model to simulate conditions under the Holstein aquitard.

Flow and transport simulations were made with MODFLOW-2005 (Harbaugh, 2005) and MT3DMS (Zheng et al., 2012), a three-dimensional finite-difference groundwater model developed by US Geological Survey. In this study the FloPy python software package (Bakker et al., 2016) was used for pre- and post-processing and simulation of MODFLOW-based models. SEAWAT (Langevin et al., 2007) was used to simulate density-dependent flow.

At the waterworks Friedrichshagen K-gallery, there are several factors influencing the state of the system. Water from the riverbank and nearby water bodies act as discharge points for groundwater in natural state conditions, and as sources of water during groundwater abstraction. Water from deep in the aquifer is the source of water and salt for our study. Model boundary conditions are based on measured and observed field conditions within the study area. The model concept simulates sinks and sources of water including: the river, other distant surface water bodies through general head, groundwater recharge, abstraction wells, and deep inflows through the constant head (Figure 1).

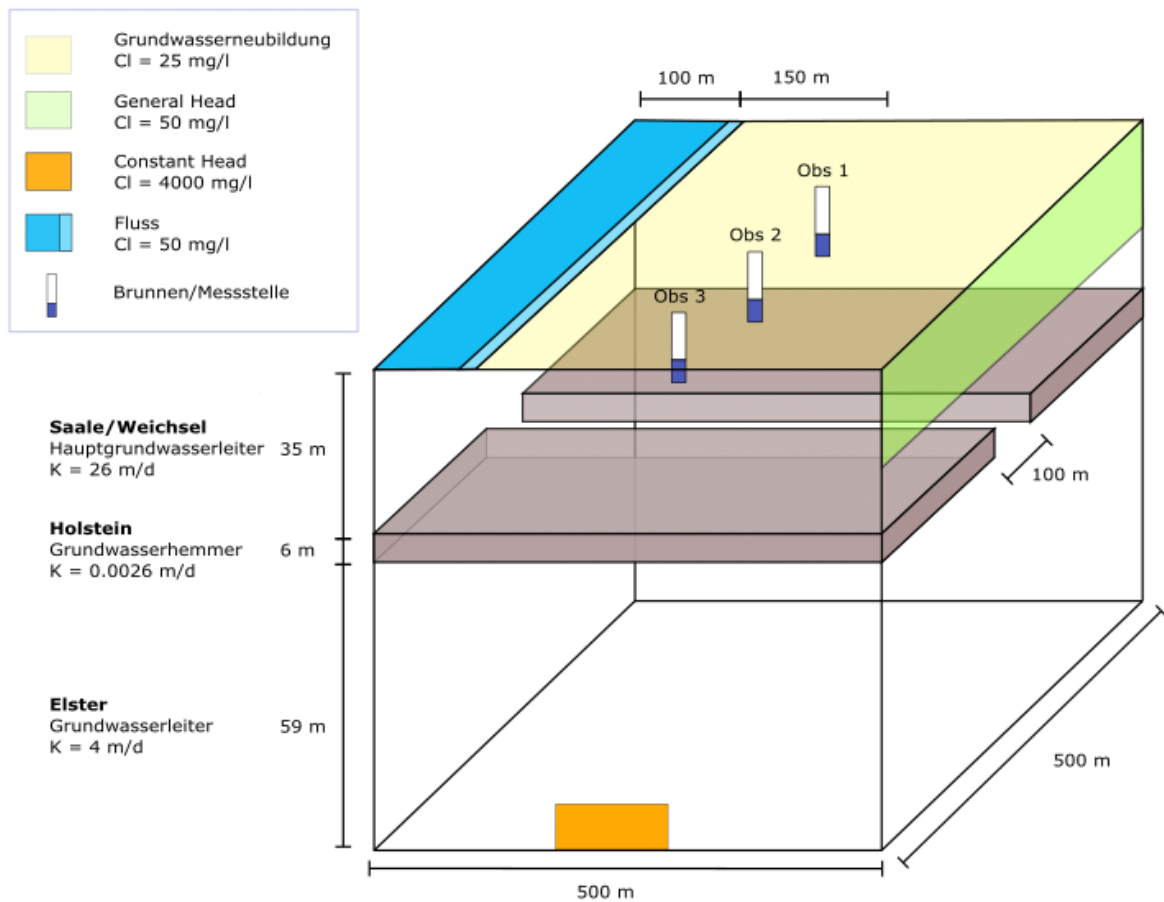


Figure 1: Schematic overview conceptual model

Water flows from local recharge into the river and regional groundwater system and deep water flows up towards the river along a low hydraulic gradient. However, the local recharge flux inhibits the majority of salt from rising above the aquitard. During groundwater extraction, the deep salt and water cross the aquitard and move towards the wells.

The model is constructed as a two-layer aquifer. The dimensions are 500m long by 500m wide and 100m in depth. Model parameters use in the base model run are presented in Table 1.

Table 1: Model Parameters

Parameter	Symbol	Value	Unit
Model Width	B	500	m
Model Length	L	500	m
Model Depth	T	100	m
Starting Head	$h_0$	0	m
Horizontal Hydraulic Conductivity (upper aquifer)	$K_{1,h}$	26	$m d^{-1}$
Vertical Hydraulic Conductivity (upper aquifer)	$K_{1,v}$	2.6	$m d^{-1}$
Horizontal Hydraulic Conductivity (lower aquifer)	$K_{2,h}$	4	$m d^{-1}$
Vertical Hydraulic Conductivity (lower aquifer)	$K_{2,v}$	0.4	$m d^{-1}$
Effective Porosity	$\varphi$	0.3	-
Well Filter Length	FL	6	m
Filter Depth Side Wells	$FOK_S$	15-21	m
Filter Depth Center Wells	$FOK_M$	15-21	m
Specific Storage Coefficient	$S_s$	$5 \cdot 10^{-4}$	$m^{-1}$
Longitudinal Dispersivity	$\alpha_L$	10	m
Transversal Dispersivity	$\alpha_T$	1	m
Cl Concentration in Recharge Water	$Cl_{rch}$	0.025	$kg m^{-3}$
Cl Concentration in River Water	$Cl_{riv}$	0.05	$kg m^{-3}$
Cl Concentration Constant Head	$Cl_{chd}$	4	$kg m^{-3}$
River Width	FB	100	m
Riverbed Depth	FT	3	m
River Stage	FH	0	m
River Bank Conductance	$FL_U$	8.6	$m d^{-1}$
River Bed Conductance	$FL_Z$	0.19	$m d^{-1}$
Abstraction Side Wells (1,3)	$Q_1, Q_3$	410	$m^3 d^{-1}$
Abstraction Center Well (2)	$Q_2$	380	$m^3 d^{-1}$
Groundwater Recharge	GRW	100	mm/a
Constant Head	CHD	0.05	m
General Head	GHB	0	m

### 3.1. Hydraulic conductivity

The upper aquifer represents the main aquifer in Berlin (Saalian and Weichselian) according to the classification from Limberg and Thierbach (2002). Hydraulic conductivity for the upper aquifer was set to 26 m/d ( $3 \times 10^{-4}$  m/s). The lower aquifer represents the aquifers 3 and 4 (Elsterian) according to Limberg and Thierbach (2002).

Measurements of hydraulic conductivity in quaternary sands originating from the Elsterian glacial period for fine to medium grain sizes was performed by Cai et al. (2015a). The authors developed a laboratory method for the determination of multi-directional hydraulic conductivities in fine-to-medium sand sediments. The range of horizontal hydraulic conductivity in these sediments ranged from 2 to 30 m/d (Cai et al., 2015a). In the base model, hydraulic conductivity for the lower aquifer is set to 4 m/d. Values from this study are also in agreement with the above mentioned classification (Limberg and Thierbach, 2002). Anisotropy is assumed as a ratio of 10 to 1. Aquifer media as presented in the model is horizontally homogeneous, save for the Holstein aquitard, which is orders of magnitudes less permeable (0.0026 m/d), having a 100m discontinuity in which hydraulic conductivity is equal to the upper aquifer.

### 3.2. Well design and abstraction rates

The well screens at the K-well field were installed from 17 to 23 meters on average under the surface of the ground. It was operated from 1984-1997 and 2008-2022 before well reconstruction. Hence, the K-gallery was effectively in operation for 27 years. During that time the well field consisted of 20 wells. Based on the long-term data (1984-1997 and 2008-2021) the average single well abstraction was around 400 m<sup>3</sup>/d. Abstraction from wells is set to 410 m<sup>3</sup>/d for the well 1 and 3 and 380 m<sup>3</sup>/d for well 2 to be consistent with the long-term average values.

The well depths and abstraction used in the base model are set to average values. Well depths are set to 15 to 21 m u GOK (see Annex Table 7 for well design).

### 3.3. Constant head

A constant head boundary is used to approximate deep saline water inflow into the model. Head measurements and density corrections using PHREEQC for hydraulic head established an upward hydraulic gradient in the study area. The constant heads at the inflow boundary are based on the moderate upward gradient apparent in the density corrected head data. Head corrections for changes in density are done using the following equation (Post and Simmons, 2022):

$$h_f = z_i + (h_i - z_i) \frac{\rho_i}{\rho_f}$$

where:

$h_f$  = equivalent freshwater pressure head, e.g. masl

$h_i$  = measured head in well

$z$  = filter elevation, e.g. masl

$\rho$  = water density; f = fresh; i = saline

For solute transport calculations, constant head cells are also set to have a constant concentration  $C_0$ . It is important to note that this approach assumes that the inflow and outflow of the solute are constant over time. Chloride concentration ( $C_0$ ) is set to 4000 mg l<sup>-1</sup> is based on measurements in

groundwater observation wells at the field site. The highest Cl value measured in FRI607UP in ~100 m depth below ground surface at the southernmost point of the K-gallery was used.

### 3.4. River package

The MODFLOW river package is used to represent the Dahme River bordering the K-gallery to the west. In the river package, the exchange flux  $Q_{riv}$  from the river to the aquifer is calculated using:

$$Q_{riv} = C_{riv}(H_{riv} - h); h > B_{riv}$$

where:

$C_{riv}$	=	<i>river bed conductance</i>
$H_{riv}$	=	<i>river stage</i>
$h$	=	<i>hydraulic head in the river cell</i>
$B_{riv}$	=	<i>bottom of the riverbed</i>

The exchange flux is negative when the hydraulic head is greater than the river head, resulting in a hydraulic gradient directed towards the river, and therefore gaining river conditions. The river bed conductance ( $C_{riv}$ ) of a given section is determined by the following equation (Harbaugh, 2005):

$$C_{riv} = \frac{K_{riv}W_{riv}L_{riv}}{d_{riv}}$$

where:

$k$	=	<i>hydraulic conductivity of the river bed sediment</i>
$w$	=	<i>width of the river cell</i>
$l$	=	<i>length of the river cell</i>
$d$	=	<i>vertical thickness of the river bed sediment</i>

Local studies have shown that the central bed and bank sediments of lakes and other water bodies in Berlin are known to have heterogeneous characteristics, due to a layer of sapropel (german: Mudde) on the central river bed acting as a hydraulic barrier (Groß-Wittke, 2014; Massmann et al., 2008b). Consequently, this study represents the heterogeneous distribution of the poorly permeable sapropel by setting two river conductance ( $C_{riv}$ ) values. The riverbank is representing by moderately clogged medium to coarse sand (hydraulic conductivity of 2.6 m/d) and the central river bed is represented by the sapropel and virtually impermeable with 0.19 m/d.

The river bottom is assigned to measured bathymetric depths from (SenStadt, 2005), where the riverbanks have 1 m and the central river bed is assigned to an average value of 3 m river water depth.

The river stage was set to the model top and varied in scenario 5. River stage measurements in Schmöckwitz at the Dahme River from 2014 – 2023 show variation of  $\Delta h = 0.005\text{m}$  (from approx. 32.39 masl in winter and 32.34 masl in summer (wasserportal.berlin.de)). By looking at historical river stages, a different picture emerges. Hasch (2024) investigated the changes in surface water levels in the Spree-Dahme system in the 19th century and the resulting consequences for the water balance, especially for the moors and wetlands. The author reported that the construction of the “Mühlendamm” led to a considerable increase of approx. 1.7 m in the Köpenicker Spree and

Dahme and resulted in the formation of alluvial flooding and marsh lands in the investigation area (Hasch, 2024).

Measurements in the Langer See (Dahme River) of riverine salt concentrations in the study area range between 44 and 57 mg l<sup>-1</sup> (average 50 mg l<sup>-1</sup>; see Table 6 in Annex 1). In recognition of this, chloride concentrations are set to 50 mg l<sup>-1</sup> for water flowing in from the river boundary.

### 3.5. Groundwater recharge

Groundwater recharge is based on water balance model for Berlin ABIMO 3.2. The program was originally developed by the Federal Institute of Hydrology and adapted to urban conditions. At the study area the groundwater recharge is given with >50-100 mm/a (SenUVK, 2019). The base model is set to 100 mm per year.

In addition to the ABIMO model, the hydrological modelling system ArcEGMO© (Becker et al., 2002) is also available. It is based on meteorological input variables and simulates the area's water balance, runoff components and watercourse discharge, considering the area's characteristics. In principle, the level of groundwater recharge calculated by ABIMO model is considered realistic and plausible. However, the recharge rates calculated for forest areas are considered to be elevated compared to e.g. ArcEgmo based simulations.

Chloride concentrations in rainfall typically range from 0 to 60 mg l<sup>-1</sup> (Scheytt, 1997). In Berlin the lowest measured values for chloride in groundwater are 25 mg l<sup>-1</sup>. Hence, groundwater recharge was attributed to Cl of 25 mg l<sup>-1</sup>.

### 3.6. General head

Besides the Dahme River, the study area is influenced by the lake Große Krampe on the eastern side. The General-Head Boundary (GHB) package is used to simulate the influence of the Große Krampe based on head-dependent flux boundaries. The GHB allows groundwater to flow either in or out of the model domain, depending on groundwater gradients along the boundary. The GHB is distinct from both a constant head and a river boundary as it considers hydraulic conductivity and distance from a given boundary. The GHB conductance ( $C_{GHB}$ ) is determined by the following equation (Harbaugh, 2005):

$$C_{GHB} = K_{GHB} * w * \frac{l}{d} \quad \text{Eq. 5}$$

where:

$K_{GHB}$	=	average hydraulic conductivity
$w$	=	thickness of the saturated aquifer perpendicular to the flow direction
$l$	=	cell length perpendicular to the flow direction
$d$	=	distance from the general head boundary to the model boundary

To approximate surface water bodies outside of the boundary area, the GHB is set with a uniform length of 500m based on the average distance to Große Krampe. Concentration from the GHB boundary are also set to 50 mg/l (Table A1.4).

### **3.7. Model discretization and transport properties**

Longitudinal and transverse dispersion were varied in the model during preliminary runs and final values of 10 m for longitudinal dispersivity and 1m for transverse dispersivity were selected based on values from a previous study (Cai et al., 2015b). Starting chloride concentrations were based on measurements from field campaigns, with 0.05 kg/m<sup>3</sup> above the Holstein window and 1 kg/m<sup>3</sup> below it.

All simulations were performed as transient flow using the TVD advection solver, which is mass conservative, without excessive numerical dispersion and artificial oscillation (Zheng and Bennett, 2002). For flow simulation, the model is set to run in the steady-state and then transport model run set to 40 years. Using this small  $\Delta t$  values can ensure that Courant number (Cr) correspondingly remained  $\leq 1$  with all different  $\Delta x$  values for minimization of numerical dispersion and oscillation (Zheng and Bennett, 2002).

### **3.8. Scenario description**

Once a model is run under natural gradients (non-pumping model), concentration plots and breakthrough curves are generated with the model output data using Python and R. Table 2 presents the parameter for each model scenario.

Table 2: Model Scenarios overview

Scenario No.	Scenario Name	Description	Parameter		
			Q <sub>1,3</sub> [m <sup>3</sup> /d]	Q <sub>2</sub> [m <sup>3</sup> /d]	Q <sub>tot</sub> [m <sup>3</sup> /d]
1.1	Varied spatial abstraction	Constant total abstraction with variable spatial abstraction between the wells	600	0	1200
1.2			550	100	1200
1.3			500	200	1200
1.4			450	300	1200
1.5*			410	380	1200
1.6			400	400	1200
2.1	Varied total abstraction	Variable total well abstraction but constant well field distribution	102.5	95	300
2.2			136.5	127	400
2.3			205	190	600
2.4*			410	380	1200
2.5			615	570	1800
2.6			820	760	2400
			<b>K<sub>1</sub> [m/d]</b>	<b>K<sub>2</sub> [m/d]</b>	<b>rK1/K2</b>
3.1	Varied hydraulic conductivity	Changing hydraulic conductivity in the lower aquifer	26	2	13
3.2*			26	4	6.5
3.3			26	6	4.3
3.4			26	8	3.25
3.5			26	10	2.6
			<b>GWN (%)</b>	<b>GWN (mm/a)</b>	<b>GWN (m<sup>3</sup>/d)</b>
4.1	Varied groundwater recharge	Constant abstraction, variable groundwater recharge	50 %	50	34.2
4.2			75 %	75	51.4
4.3*			100 %	100	68.5
4.4			125 %	125	85.6
4.5			150 %	150	102.7
			<b>Δ River Stage</b>		
5.1	Change in river stage	Constant abstraction, variable river stage in riverbank and the general head boundary	- 0.05 m		
5.2			- 0.025 m		
5.3*			0 m		
5.4			+ 0.025 m		
5.5			+ 0.05 m		

\*base model settings

## 4. Results

### 4.1. Non-pumping model

Chloride concentration over time is illustrated by two profile sections, in north-south and west-east direction, each through the center of the model (Figure 2).

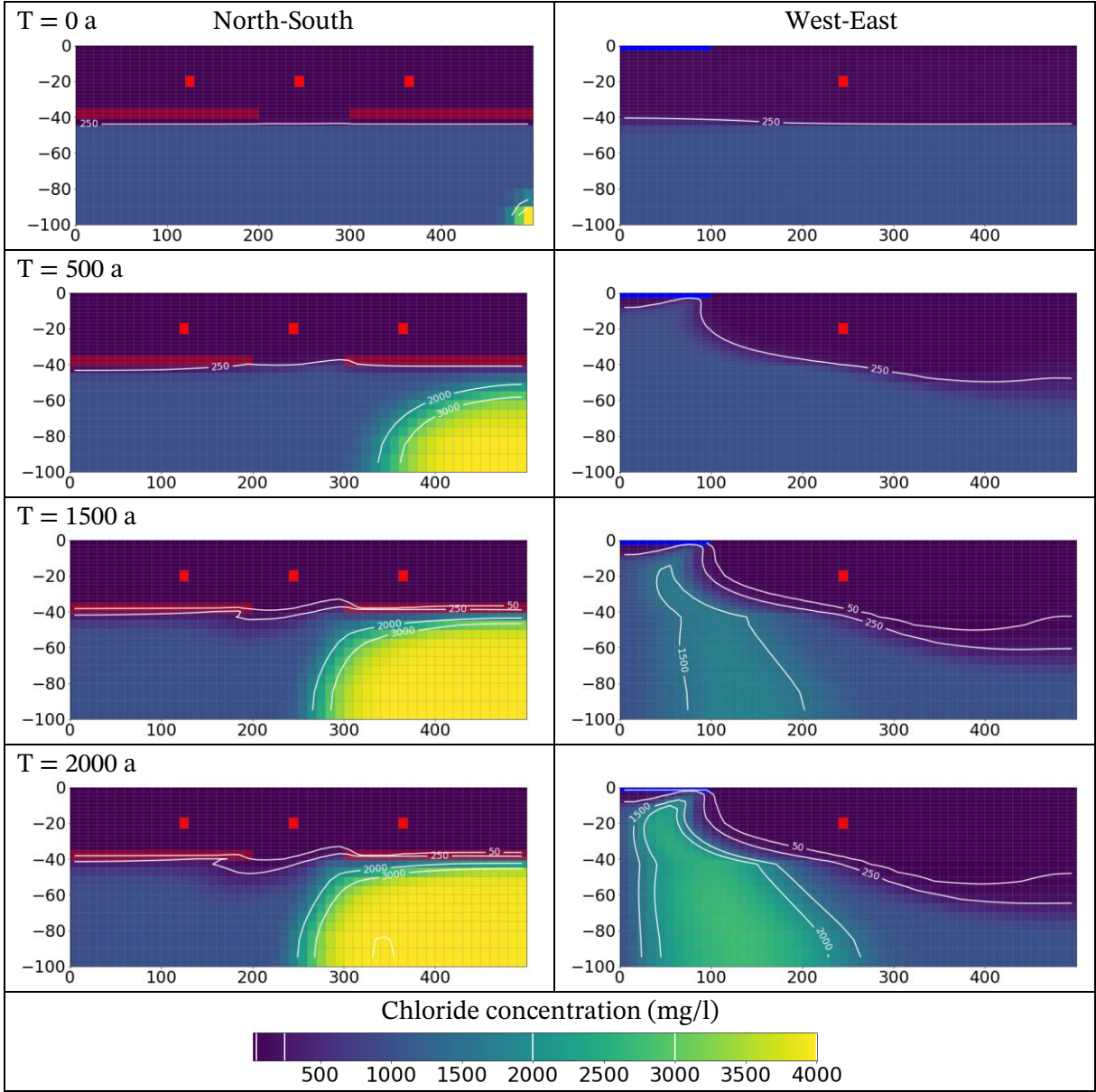


Figure 2: Simulated chloride concentration cross-sections at T = 0, 500, 1000, 1500 and 2000 years (red dots = observation cells; blue line = river cells; brown layer = Holstein aquitard cells)

The non-pumping simulation start with a homogeneous chloride concentration of 50 mg/l and 1000 mg/l in the upper and lower aquifer, respectively. At  $T = 0a$  the two aquifers are separated by horizontal stratification of chloride concentration. After 2000 simulated years the chloride concentration were found to be in quasi-equilibrium state.

During non-pumping simulation, chloride concentration from the constant head boundary (see section 3.3 for details) is developing over time moving from the south up towards the river. In the west-east profiles, the development of a salt plume below the river can be well observed. The river acts as a hydraulic discharge under natural gradient, so that more and more salt accumulates. However, a small freshwater pocket of few meters remains at the western model edge directly below the river. This is due to the low permeability sapropel layer formed there. On the riverbank, the sapropel is not present and the salt can reach the river (see section 3.4 for details). This finding is in line with observations of the first known test drillings at the north-east of "Langer See" from the 1930s (Anonym, 1940). The drilling report states that the groundwater at a depth of about 60 m below ground has a chloride concentration of about 1500 mg/L (Anonym, 1940). Consequently, the authors concluded that the groundwater in this area is unsuitable for drinking water production. Compared to the findings of the first exploratory drillings, simulated concentration, e.g. after 1500a of natural state, are similar to the measurements done in the 1930s.

The chloride builds up under the Holstein aquitard in the south and west portion of the model and advances and disperses a few meters under the central observation point. After a 2000-year model run with constant boundary conditions a state is reached with plausible stratification according to measurements from our sampling campaign. The concentrations effectively represent natural conditions, especially the distribution of salt below the Holstein aquitard. Salt distribution evolves over long periods of time due to the effect of hydrodynamic dispersion and advection.

Groundwater recharge is the dominant inward flux and discharges either west or east towards the GHB or RIV boundary conditions. Approx. two cubic meters of water enters the model per day from the constant head boundary, increasing salt concentrations gradually within the model region over time (Table 3).

Table 3: Water balance for non-pumping scenario

Flux	Units	IN	OUT
Storage	$m^3d^{-1}$	3.31	0
Constant Head Boundary	$m^3d^{-1}$	2.09	0
Wells	$m^3d^{-1}$	0	0
River	$m^3d^{-1}$	0	71.27
General Head Boundary	$m^3d^{-1}$	0	3.18
Recharge	$m^3d^{-1}$	68.49	0
Total	$m^3d^{-1}$	73.89	75.72
Percent Discrepancy	-	0.75%	0.76%

Plots of hydraulic heads show the magnitude and relative importance of the model hydraulic gradients. Overall, the river exerts the most influence over the flow of groundwater in the region above the Holstein window. Figure 3 presents the distribution of hydraulic heads and corroborates the results from the water budget. In these conditions, the influx of recharge water has a visually significant effect in the upper regions of the model, but the highest hydraulic gradient comes in from the south.

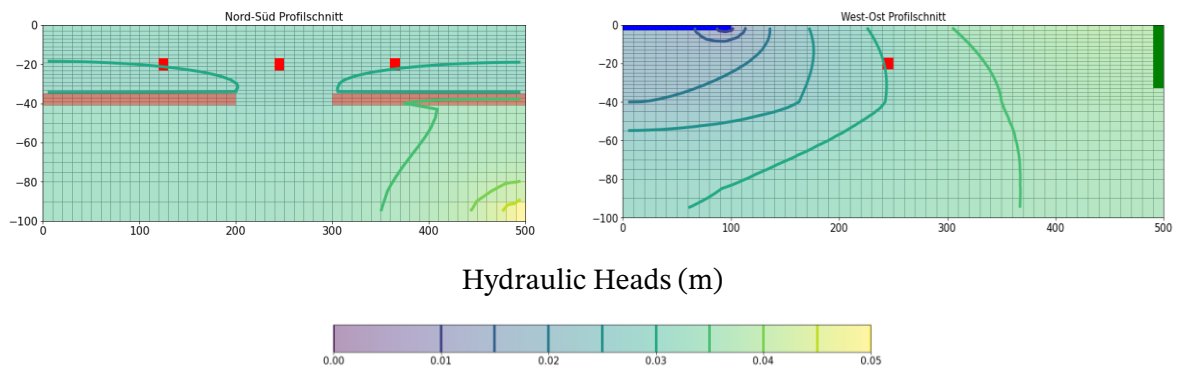


Figure 3: Cross sections of hydraulic heads non-pumping scenario

## 4.2. Base model

The base model pumping conditions are designed to represent the initial activation of wells after the first commissioning in 1984. The base model represents a model that calculates with long-term average pumping rates and parameters as shown in Table 1. The position of observation/abstraction wells in the base model corresponds to the filter screen depths before well reconstruction (see section 3.2 for details). Simulation period is set to 40 years under constant pumping stress. This period is longer than the effective period of operation from the start of commissioning to the new construction of the well field in 2022/23. (Figure 4).

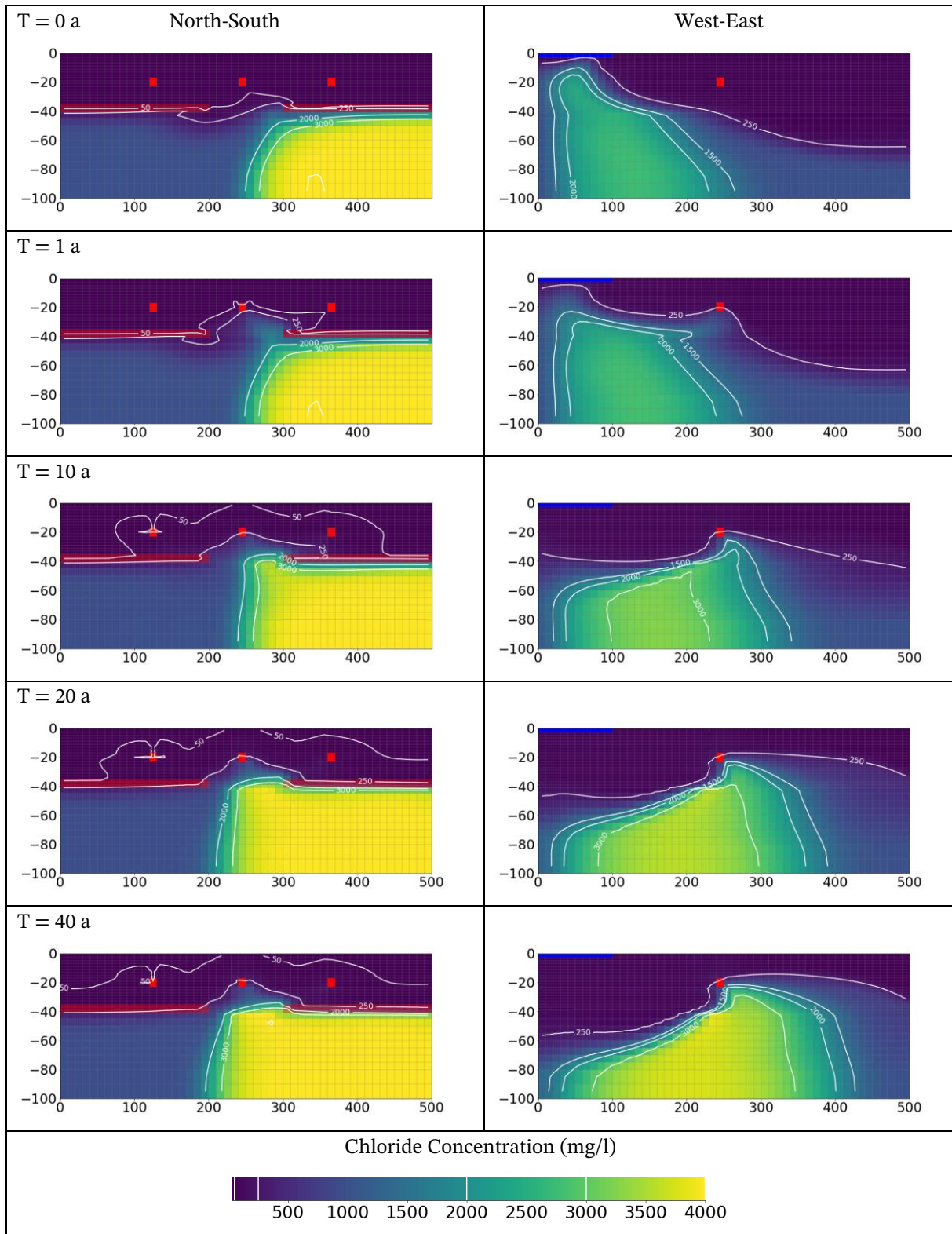


Figure 4: Simulated chloride concentration cross-sections at T = 0, 1, 10, 20 and 40 years of pumping (red dots = observation/abstraction well cells; blue line = river cells; brown layer = Holstein aquitard cells)

The simulated chloride concentrations during pumping are strongly influenced by the starting concentrations used. Measurements of the spatial distribution of chloride in the study area before the beginning of groundwater abstraction are scarce. There are only a few measurements available from a borehole drilled in the 1930s (Anonym, 1940), as discussed above. It is therefore not possible to specify the spatial distribution of chloride concentrations as start conditions in detail. Instead, the simulation results of the non-pumping model are used as the initial starting conditions. Based on the simulated chloride concentration from the non-pumping scenario the time step  $T = 2000a$  was used as an initial condition for pumping scenarios.

The temporal development of the simulated chloride concentrations and the cumulated chloride loads in the wells are shown in Figure 5. The chemical load was calculated by multiplying the simulated concentration by the well withdrawal for each well and then presented cumulatively.

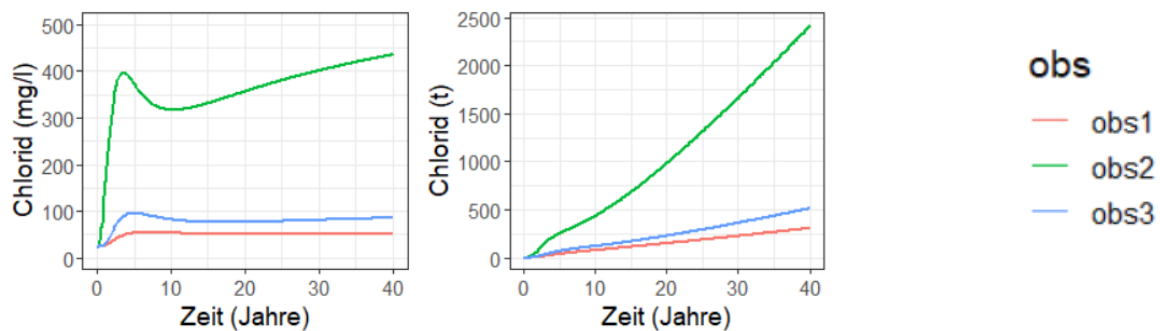


Figure 5: Breakthrough curves concentration vs. time (left); cumulated load of chloride vs. time (right)

The simulated chloride as shown in Figure 5 and Figure 4 corresponds to measured trends in hydro chemical evolution at the K-well field:

1. The highest chloride concentration simulated in the central well is approx. 450 mg/l after 40 years of pumping. This is in the same order of magnitude as measured maximum concentrations from the K-well field, e.g. measured chloride in 2018 was about 400 mg/l in well#8 (see Annex Figure 15).
2. Simulated concentration in the well 2 and 3 rise to a maximum within a few years and then fall again within 10 years of active operation. This behaviour is not observed in well 1, because it is furthest away from the CH boundary in the south. This “early peak behaviour” agrees well with measured chloride at the K-gallery. In the first years of well operation in the 1980s, an increase and, after some time, a decrease of the salt concentrations in the wells was observed (Emshoff, 1991). The measured chloride values rose from below 100 mg/l to almost 400 mg/l in some wells, only to drop again to 100-150 mg/l within 10 years (see Annex Figure 16).
3. The simulated steady increase over time in concentration in the central well after the initial peak is reflected by measured data (see Annex Figure 17 and Figure 18).

Simulated Cl concentrations do not reach a steady-state equilibrium after 40 years of pumping. When simulation is extended up to 100 years, chloride concentrations in the model still has not reached equilibrium. The other two wells show no or marginal increase. However, the increase in the curve is flattened and the Cl concentrations in the central well are around 550 mg/l. Due to the flattened curves in central well, a chloride concentration of more than 600 mg/l is not to be expected.

For OBS 1, 2, and 3 respectively after the model is run for this extended time period. model water budgets can provide insight on the maximum mobilization of salt in the system. Constant head water inflow amounts to 58.8 m<sup>3</sup>/d providing a theoretical maximum of 85 tons per year (t/a) of chloride. Calculated this way, the river, GHB, and recharge boundary conditions contribute another 20 t/a into the model boundary. Therefore, based on these boundary conditions (and their respective constant concentrations), the maximum yearly salt load for this model realization is 105 t/a.

Model water budgets, presented in Table 4, show an increase in the amount of water flowing through the system to match well extraction. The river boundary contributes 85% and the GHB contributes 4% of the water input. Isotope tracer studies done to determine the share of bank filtrate at the K gallery determined a mean value of 68% for the bank filtrate fraction, with an upper and lower tail of 77% and 60%, respectively (Altmannsberger, 2018). Numerical model simulation of the share of bankfiltrate in the K-gallery found values of 86-92% (DHI-WASY, 2017). Due to the dominance of the river and GHB margins in the model, the influence of the bank filtrate is therefore compared to the isotope study somewhat overestimated, but consistent with the large scale numerical model and within a plausible range.

Table 4: Water balance base model

Flux	Inflow [m <sup>3</sup> d <sup>-1</sup> ]	Outflow [m <sup>3</sup> d <sup>-1</sup> ]	Percent Discrepancy
Storage	4.8	0	
Constant Head Boundary	58.8	0	
Wells	0	1200	
River	1023.1	0	
General Head Boundary	44.1	0	
Groundwater Recharge	68.4	0	
Total	1199	1200	-0.11%

Plots of hydraulic heads presented in Figure 6 show the wells exert a large area of influence within the model, drawing water from all boundary conditions.

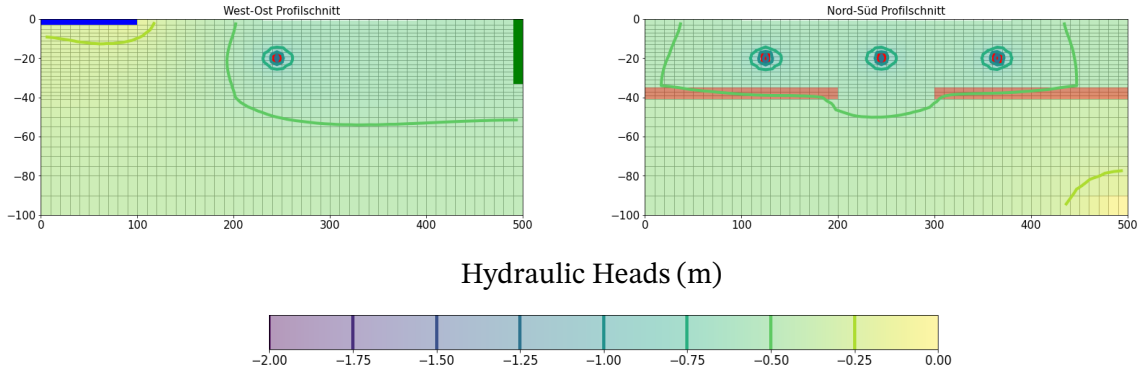


Figure 6: Cross sections of hydraulic heads for base scenario

Many studies have shown that water density variations exert an important control on groundwater movement (Post and Simmons, 2022). Hence, numerical modeling was also performed accounting for variable-density flow by using SEAWAT-2000 (Langevin et al., 2007). SEAWAT-2000 is a coupling of the MODFLOW groundwater flow code, modified to solve variable-density flow conditions using equivalent freshwater head, with the MT3DMS transport model. This was done to check whether density-dependent transport has an influence on the simulated results. The simulated breakthrough curves differ in the first 10 years, during the "early peak behaviour", but after approx. 10 years of simulation no significant difference can be observed (Figure 7).

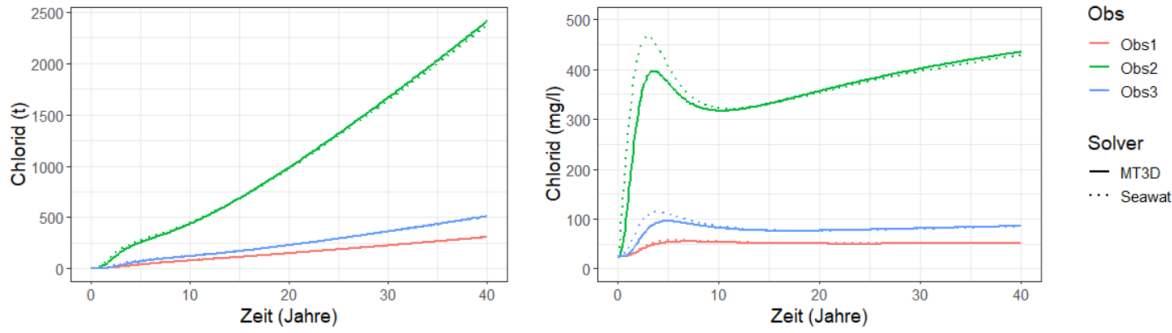


Figure 7: Comparison SEAWAT with MT3D solution

Density-dependant flow between seawater and freshwater with a distinct salt-/freshwater hydrochemical difference. The maximum chloride concentration in this study is defined by 4000 mg/l at the salt interface and 50 mg/l at the freshwater boundaries. There is about 19400 mg/L chloride in seawater. This means that the highest concentration in this study is more than four times lower than seawater.

### 4.3. Scenario group 1

Within this scenario group, the total groundwater abstraction remains constant ( $Q_{\text{tot}} = 1200 \text{ m}^3/\text{d}$ ) but the amount extracted at each well is varied. Six model runs were conducted, with the extraction at the central well 2 starting from  $0 \text{ m}^3/\text{d}$  and extraction at the wells 1+3 of  $600 \text{ m}^3/\text{d}$ . The extraction at the central well is then increased to 100, 200, 300, and finally to  $400 \text{ m}^3/\text{d}$  while extraction at the well 1+3 is decreased stepwise to maintain a total extraction of  $1200 \text{ m}^3/\text{d}$  (see Table 2). Detailed information for each scenario, including breakthrough curves of concentration vs time and cumulated load of chloride for each simulation run is shown in annex 2 (Figure 21, Figure 22, Figure 23, Figure 24, Figure 25).

The results of these runs encapsulate the effect of varying abstraction in wells directly over aquitard discontinuities change the amount of salt seen in wells. In this scenario group, the function of the central well as a defence well is investigated. A defence well is intended to intercept pollutants from the groundwater to prevent them from entering the drinking water. The central well should prevent most of the salt from reaching the neighbouring wells and spreading in the aquifer. However, it can be assumed that an increase in well abstraction directly above a Holstein window can lead to a disproportionate increase in the salt load.

Concentrations are shown as box plots, where the length of the box ranges from the 25<sup>th</sup> percentile and the 75<sup>th</sup> percentile. Lines that extend beyond this box is defined by the factor 1.5 to either side (Figure 8).

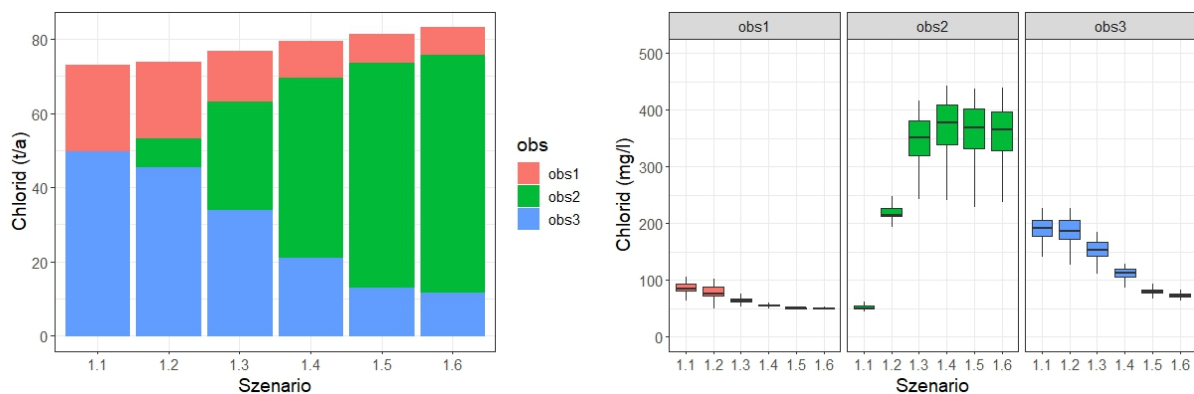


Figure 8: Mean annual load (t/a) and chloride concentration (mg/l) over 40a of pumping for scenario group 1

The stepwise increase of  $Q$  in the central well ( $Q_2$ ) and the proportional decrease in the neighbouring wells lead to an increase in the total chloride load. Chloride load with zero pumping in the central well is lowest with approx. 73 t/a, and the highest load is found in the model representing the base model with about 83 t/a. Hence, the simulations show that the increase of pumping above the Holstein window increases the mean annual chloride load by ~10 tonnes without increasing the total abstraction.

The doubling of the pumping rate in the central well (e.g. scenario 1.3 to 1.6) leads to a more than twice as much salt load, from about 30 t/a to 64 t/a. However, the simulated concentrations in the

central well remain below 500 mg/l and do not increase excessively. The simulated concentrations show that the central well protects the neighbouring wells from salt ingress.

#### 4.4. Scenario group 2

In scenario group 2, total well extraction amounts was stepwise increased from 300 m<sup>3</sup>/d to 2400 m<sup>3</sup>/d (see Table 2). In all model runs, according to the base scenario setting the central well was attributed to a 7% lower pumping rate than the neighbouring wells.

Detailed information for each scenario, including breakthrough curves of concentration vs time and cumulated load of chloride for each simulation run is shown in the annex 2 (Figure 26, Figure 27, Figure 28, Figure 29, and Figure 30).

It is clear that an increase in well abstraction leads to an increased mobilisation of deep groundwater and thus elevated salt in the wells. In this scenario, it should be investigated how the increase in the total abstraction influences the amount of bank filtrate that leads to a compensation salinity ingress in the wells (Figure 9).

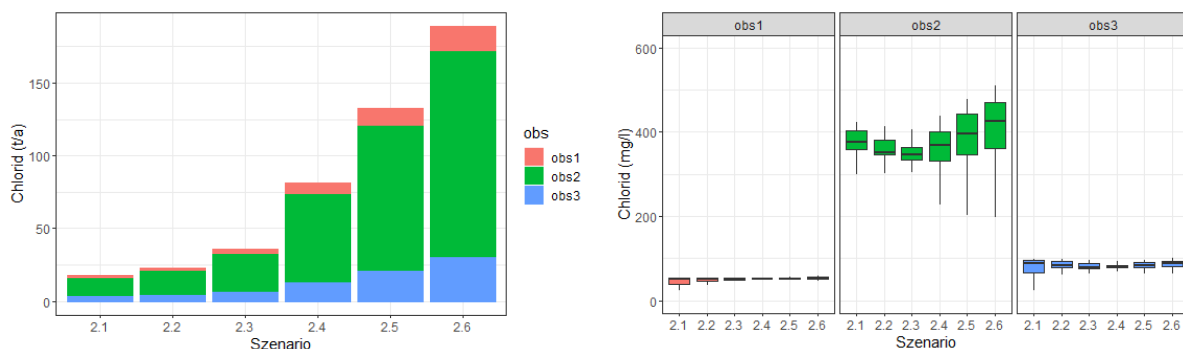


Figure 9: Mean annual chloride load (t/a) and chloride concentration (mg/l) over 40a of pumping for scenario group 2

Total chloride load increases with each increase in abstraction, from approx. 18 t/a in scenario 2.1 to 190 t/a in scenario 2.6. Doubling the well extraction in scenario 2.3 to 2.4 leads to an increase in the total salt load from approx. 36 t/a to 81 t/a. Further doubling of groundwater extraction from scenario 2.4 to 2.6 leads to approx. 189 t/a. Hence, the simulations show that there is a disproportionate increase in the salt load. This is also evident when looking at the simulated concentrations. The simulated concentrations remain in a moderate range below 600 mg/l, but increases in the central well. While the chloride concentration in the central well is rising with increased abstraction, the concentrations in the neighbouring wells appear to be relatively constant. This shows that under the given boundary conditions the central well retains its protective function even with increasing withdrawal volumes.

Simulations show that the proportion of bank filtrate in the wells increases as a result of the gradual increase in abstraction, but reaches a maximum value of approx. 92% (88% from the Langer See (river boundary) and ~4% from the Große Krampe (GHB)). Increasing groundwater abstraction leads to an increase of salt within the wells, regardless of the increase in the share of bank filtrate.

### 4.5. Scenario group 3

In scenario group three, the hydraulic conductivity of the lower aquifer was varied between plausible values from 2 to 10 m/d (for more information see section 3.1 Hydraulic conductivity). Detailed information for each scenario, including breakthrough curves of concentration vs time and cumulated load of chloride for each scenario run is shown in the annex 2 (Figure 31, Figure 32, and Figure 33).

It is clear that the higher the hydraulic conductivity in the lower aquifer is, the higher the simulated salt concentration and load will be. The question in this scenario was to what extent the natural heterogeneities may influence saltwater migration. Simulations show that although the hydraulic conductivity of the lower aquifer have changed by a factor of 5 only, the loads and concentration react very sensitively and chloride concentration in the central well can reach values of up to 1000 mg/l (Figure 10).

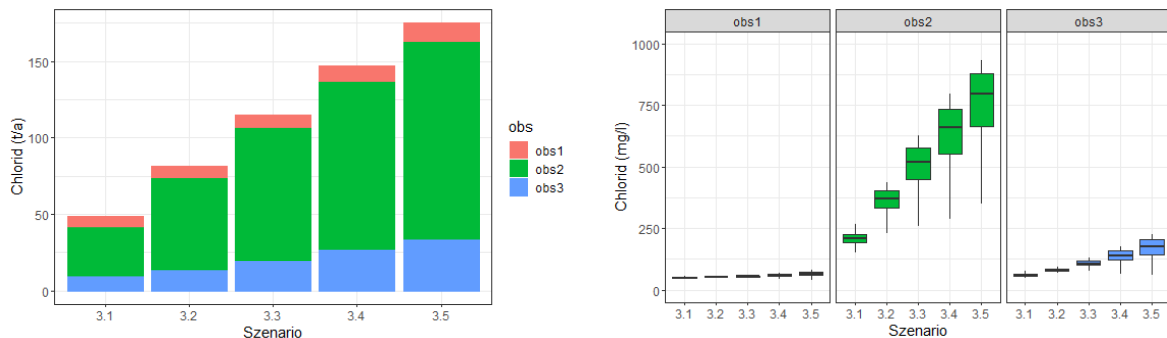


Figure 10: Mean annual chloride (t/a) and chloride concentration (mg/l) over 40a of pumping for scenario group 3

The doubling of the hydraulic conductivity (e.g. scenario 3.1 to 3.2, or 3.2 to 3.4) in the lower aquifer leads to a salt load increase of approx. 70%. Riverbank filtrate in wells drops by nearly 10%, from 87% to 79% in scenario 3.1 to 3.5 respectively.

In the scenario with the lowest hydraulic conductivity (scenario 3.1), inflow from the constant head boundary drops to half of the base model. With the highest hydraulic conductivity (scenario 3.5), inflow from the lower boundary increases to over twice that of the base model.

#### 4.6. Scenario group 4

In scenario group 4, groundwater recharge was varied from 50 to 150 percent of the original groundwater recharge. A detailed description of the results of all model runs can be found in the annex 2 (Figure 35, Figure 36, Figure 37, and Figure 38).

In the base model, groundwater recharge makes up 6% of the model inflow and the groundwater system is dominated by the influence of bank filtrate from the river and the GHB boundary, and inflow from the constant head boundary. The model domain is therefore smaller than the well gallery catchment area in nature would actually be. However, the K-gallery is dominated by bank filtrate from two sides (Langer See and Große Krampe). Compared to other studies (see section 4.4 for details) the influence of groundwater recharge is somewhat underestimated, but consistent with the large scale numerical model (DHI-WASY, 2017) and within a plausible range.

The fraction of bank filtrate decreases slightly (from 7 to 5 %) from scenario 4.1 to 4.5. Therefore, salt load and concentrations do not vary significantly in these scenarios (Figure 11).

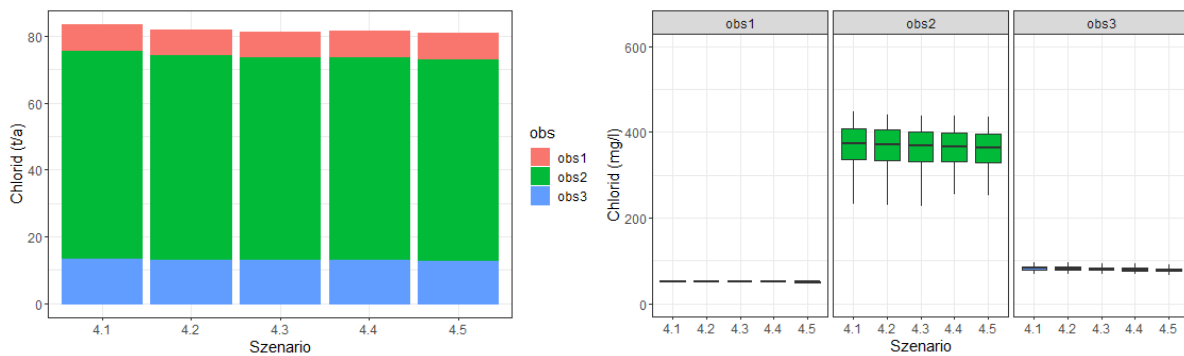


Figure 11: Mean annual chloride load (t/a) and chloride concentration (mg/l) over 40a of pumping for scenario group 4

### 4.7. Scenario group 5

In scenario group 5, river stage of the river boundary and the GHB boundary was varied from 5 cm below to 5 cm above the model top elevation. A detailed description of the results of all model runs can be found in the annex 2 (Figure 39, Figure 40, Figure 41, and Figure 42).

It is obvious that an increase in water levels causes greater hydraulic gradients between surface water and groundwater and leads to higher bank filtrate fractions and thus lower saltwater influence. In this scenario, it is investigated to what extent the surface water level influences the salt ingress in the wells. Compared to base scenario (s5.3) a lowered river stage of -5 cm (s5.1) results an increase of chloride concentration and load in the central well of approx. 70 mg/l and 9 t/a, respectively. An increase of +5 cm (s5.5) results in a similar change, but decrease of chloride concentration and load in the central well of approx. 60 mg/l and 8 t/a, respectively (Figure 12).

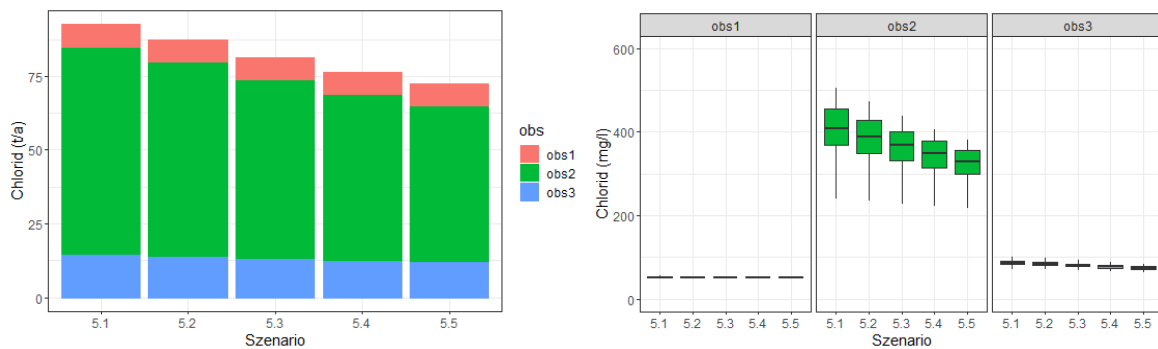


Figure 12: Mean annual chloride load (t/a) and chloride concentration (mg/l) over 40a of pumping for scenario group 5

In these simulations, it is noticeable that even small changes in the water levels of a few centimetres lead to relatively large changes in the salt concentrations and loads in the wells. It follows that the surface levels are a sensitive parameter for salt migration in well fields influenced by bank filtrate.

## 5. Conclusions

The simulations in the non-pumping model make clear that the transport processes in the deep geological subsurface require thousands of years to reach a quasi-equilibrium state. In contrast to the model, boundary conditions in nature are not stable over long periods of time. Therefore, the observed conditions in nature must be considered as a transient state of non-equilibrium.

The base model is capable to simulate the trends in hydrochemical development observed in the wells. As a result, a model-based explanation for the hydrochemical development of the past could be developed for the first time.

From scenario 1, it can be concluded that the central well protects the neighbouring wells from salt ingress, but increases the annual abstracted salt load by ~10 tonnes. Under the given conditions, however, the simulations did not show an excessive increase of salt loads. The function of the central well as a defensive well to prevent the spread of saline groundwater in the upper aquifer was confirmed by the simulations. The current practice of operating the central well at a lower pumping rate compared to the neighbouring wells proves to be effective.

The simulations in scenario 2 show a disproportionate increase in salt loads with increasing withdrawals from the groundwater, which cannot be compensated by the bank filtrate. It can be concluded, that bank filtration is limited by the hydraulic connection of the riverbed. Other studies have shown that deeper areas of rivers in Berlin are characterized by low conductive sediments with high deposition of organic material which results in lower infiltration rates (Groß-Wittke, 2014; Massmann et al., 2008a; Massmann et al., 2008b). Only the shallow littoral zones can be considered relevant for bank filtration, as this area is kept permeable by waves and meiofauna activity. This heterogeneous distribution of the infiltration zone leads to a restriction of the bank filtrate and is simulated realistically in the model. However, the the central well retains its protective function even with increasing withdrawal volumes. Further increases in total withdrawals are at the expense of the groundwater storage and a gradual increase of salt in the wells.

Simulation runs in scenario 3 shows the strong dependence of the salt transport on the hydraulic conductivity. Simulations show that the natural heterogeneities of hydraulic conductivity in the geological subsurface can lead to a sharp increase in salt concentrations and loads. In the central well, chloride concentrations were simulated that were far above the drinking water limit and would pose considerable difficulties for the operation of the well field. A hydrogeological characterization of the deep underlying subsurface is therefore indispensable, especially in places where confining layers are missing.

The change in groundwater recharge in scenario 4 has no significant influence on the simulated concentration and loads. However, this is primarily due to the boundary conditions of the model, which are primarily fed by the surface waters.

Simulations in scenario 5 show that even small changes in the water level in the Dahme River lead to significant changes in the chloride concentration in the wells. Therefore, if water levels fall below today's levels for a longer period of time, greatly increased chloride levels must be expected in the wells.

## References

- Altmannsberger, C. (2018) Multitracer-Untersuchungen zur Ermittlung der Uferfiltratanteile von Trinkwasserbrunnen am Wasserwerk Friedrichshagen (Berlin).
- Anonym (1940) Vorläufiger Bericht über das Ergebnis der Probebohrungen zur Erforschung noch vorhandener Trinkwassergewinnungsmöglichkeiten in der Umgebung von Berlin
- Bakker, M., Post, V., Langevin, C.D., Hughes, J.D., White, J.T., Starn, J.J. and Fienen, M.N. (2016) Scripting MODFLOW Model Development Using Python and FloPy.
- Becker, A., Klöcking, B., Lahmer, W. and Pfützner, B. (2002) The Hydrological Modelling System ArcEGMO, in: Singh, V.P., Frevert, D.K. (Eds.), *Mathematical Models of Large Watershed Hydrology*.
- Cai, J., Taute, T., Hamann, E. and Schneider, M. (2015a) An Integrated Laboratory Method to Measure and Verify Directional Hydraulic Conductivity in Fine-to-Medium Sandy Sediments. *Groundwater* 53, 140-150.
- Cai, J., Taute, T. and Schneider, M. (2015b) Recommendations of Controlling Saltwater Intrusion in an Inland Aquifer for Drinking-Water Supply at a Certain Waterworks Site in Berlin (Germany). *Water Resources Management* 29, 2221-2232.
- DHI-WASY (2017) Verifikation der Modellparameter für das Sulfat-Bilanzmodell des Wasserwerks Friedrichshagen.
- Emshoff (1991) GA Q30 Friedrichshagen F - M (1991), Hydrogeologisches Gutachten Berlin - WW Friedrichshagen Q30 Galerien F bis M, Berlin.
- Felsch, T. (2022) Ableitung von Empfehlungen aus Strömungs- und Strukturmodellen für den Bau und Betrieb von salzwasserbeeinflussten Brunnen am Beispiel der Brunnengalerie K des Wasserwerks Berlin-Friedrichshagen.
- Groß-Wittke, A. (2014) Effects of increasing Water Temperature on Bank filtration: Experimental Studies at Lake Tegel, Berlin, Germany, *Prozesswissenschaften*. Technische Universität Berlin.
- Grube, A. and Martens, S. (2011) Grundwasserversalzung in Deutschland.
- Grube, A., Wichmann, K., Hahn, J. and Nachtigall, K.H. (2000) Geogene Grundwasserversalzung in den Poren-Grundwasserleitern Norddeutschlands und ihre Bedeutung für die Wasserwirtschaft. *Geogenic groundwater salinisation in the pore aquifers of northern Germany and its significance for water management*.
- Harbaugh, A.W. (2005) MODFLOW-2005, the US Geological Survey modular ground-water model: the ground-water flow process. US Department of the Interior, US Geological Survey Reston, VA, USA.
- Hasch, B. (2024) Der Einfluss der gründerzeitlichen Spreeregulierung auf die Moore des Spree-Dahmesystems bei Köpenick (Berlin) - The impact of the Wilhelminian regulation of the river Spree on the mires of the Spree-Dahme river system at Köpenick (Berlin). *Berichte der deutschen Gesellschaft für Moor und Torfkunde*.
- Langevin, C.D., D.T., T.J., Dausman, A.M., Sukop, M.C. and Guo, M.C. (2007) SEAWAT Version 4: A Computer Program for Simulation of Multi-Species Solute and Heat Transport. U.S. Geological Survey *Techniques and Methods*. Book 6.
- Limberg, A. and Thierbach, J. (2002) Hydrostratigrafie von Berlin - Korrelation mit dem Norddeutschen Gliederungsschema. *Hydrostratigraphy of Berlin - Correlation with the North German classification scheme*. *Brandenburger geowissenschaftliche Beiträge* 9, 65-68.
- Massmann, G., Nogeitzig, A., Taute, T. and Pekdeger, A. (2008a) Seasonal and spatial distribution of redox zones during lake bank filtration in Berlin, Germany. *Environmental Geology* 54, 53-65.
- Massmann, G., Sültenfuß, J., Dünnbier, U., Knappe, A., Taute, T. and Pekdeger, A. (2008b) Investigation of groundwater residence times during bank filtration in Berlin: A multi-tracer approach. *Hydrological Processes: An International Journal* 22, 788-801.
- Post, V. and Simmons, C. (2022) Variable-density groundwater flow, Ontario, Canada.
- Scheytt, T. (1997) Seasonal Variations in Groundwater Chemistry Near Lake Belau, Schleswig-Holstein, Northern Germany. *Hydrogeology Journal* 5, 86-95.

- Schramm, T. and Herd, R. (2020) Geogene Grundwasserversalzung in Berlin - Geogenic groundwater salinization in Berlin. Brandenburg. geowiss. Beitr. 27, 47-60.
- SenStadt (2005) Gewässeratlas von Berlin - Von der Gewässervermessung zum Gewässeratlas von Berlin mit hydrographischem Informationssystem. Senatsverwaltung für Stadtentwicklung Bereich Kommunikation.
- SenUVK (2019) Karte 02.17 Grundwasserneubildung.
- van Weert, F., van der Gun, J. and Reckman, J. (2009) Global Overview of Saline Groundwater Occurrence and Genesis, in: report nr GP 2009-1, I.g.r.a.c. (Ed.). IGRAC, Utrecht, Netherlands.
- Zheng, C. and Bennett, G.D. (2002) Applied Contaminant Transport Modeling, Second Edition. John Wiley & Sons, New York.
- Zheng, C., Hill, M., Cao, G. and Ma, R. (2012) MT3DMS: Model Use, Calibration, and Validation. Transactions of the ASABE 55, 1549-1559.

## Annex 1: Supplementary information

Table 5: Density corrections for observed hydraulic heads during Geosalz field sampling

Station ID	Sampling date	Head <sub>unc.</sub> [m asl]	Flow Direction	Density [g cm <sup>-3</sup> ]	Bottom Pair Head <sub>corr</sub> [m asl]	$\Delta H_{corr}$ [-]	Flow Direction (corrected)
FRI603OP	30/03/2022	32.2	Down	1.0004	32.32	-0.12	Up
FRI603UP	30/03/2022	32.06		1.00323			
FRI607OP	16/05/2022	32.27	Down	1.00015	32.35	-0.08	[-]
FRI607UP	16/05/2022	31.92		1.00481			
FRI603OP	21/06/2022	32.26	Up	1.00023	32.70	-0.44	Up
FRI603UP	21/06/2022	32.44		1.00299			
FRI605OP	21/06/2022	32.23	Down	1.00002	32.36	-0.13	Up
FRI605UP	21/06/2022	32		1.00389			
FRI604OP	22/06/2022	32.26	[-]	0.99992	32.25	0.01	[-]
FRI604UP	22/06/2022	32.19		1.00104			
FRI603OP	11/04/2023	32.37	Down	1.00022	32.45	-0.08	[-]
FRI603UP	11/04/2023	32.19		1.00299			
FRI604OP	11/04/2023	32.38	[-]	0.99988	32.40	-0.02	[-]
FRI604UP	11/04/2023	32.33		1.00113			
FRI605OP	11/04/2023	32.37	Down	1	32.51	-0.14	Up
FRI605UP	11/04/2023	32.14		1.00397			
FRI2012OP	12/04/2023	32.38	Down	0.99993	32.45	-0.07	[-]
FRI2012UP	12/04/2023	32.23		1.0035			
FRI607OP	13/04/2023	32.37	Down	1.00007	32.61	-0.24	Up
FRI607UP	13/04/2023	32.17		1.00482			
FRI603OP	17/07/2023	32.22	Down	0.99986	32.26	-0.04	[-]
FRI603UP	17/07/2023	31.99		1.00284			
FRI604OP	17/07/2023	32.08	Down	0.99971	31.09	0.99	Down
FRI604UP	17/07/2023	31.03		1.00073			

Station ID	Sampling date	Head <sub>unc.</sub> [m asl]	Flow Direction	Density [g cm <sup>-3</sup> ]	Bottom Pair Head <sub>corr</sub> [m asl]	$\Delta H_{corr}$ [-]	Flow Direction (corrected)
FRI2012OP	18/07/2023	32.1	Down	0.99914	32.16	-0.06	[-]
FRI2012UP	18/07/2023	31.93		1.00293			
FRI605OP	18/07/2023	31.95	Down	0.99965	31.19	0.76	Down
FRI605UP	18/07/2023	30.83		1.00362			
FRI607OP	19/07/2023	31.97	Down	0.99993	32.19	-0.22	Up
FRI607UP	19/07/2023	31.77		1.00449			
FRI603OP	23/10/2023	32.04	Down	1.00007	32.21	-0.17	Up
FRI603UP	23/10/2023	31.93		1.00311			
FRI1008	24/10/2023	32.04	Down	0.99987	31.95	0.09	[-]
FRI606	24/10/2023	31.75		1.00352			
FRI2012OP	24/10/2023	31.96	Down	0.99992	32.03	-0.07	[-]
FRI2012UP	24/10/2023	31.84		1.00303			
FRI604OP	24/10/2023	32.14	Down	0.99976	32.06	0.08	[-]
FRI604UP	24/10/2023	32		1.0009			
FRI605OP	24/10/2023	31.91	Down	0.99985	32.13	-0.22	Up
FRI605UP	24/10/2023	31.76		1.00379			
FRI607OP	25/10/2023	32.04	Down	1	32.24	-0.20	Up
FRI607UP	25/10/2023	31.82		1.00451			

*Figure deleted for data protection reasons*

Figure 13: Well profile –K-well field 1983

*Figure deleted for data protection reasons*

Figure 14: Observed chloride concentration in K-well field vs well ID from 1983 to 1995 (BWB data)

*Figure deleted for data protection reasons*

Figure 15: Observed chloride concentration in K-well field vs well ID from 2008 to 2021 (BWB data)

*Figure deleted for data protection reasons*

Figure 16: Observed chloride concentration in K-well field vs year from 1983 to 1995 (BWB data)

*Figure deleted for data protection reasons*

Figure 17: Observed chloride concentration in K-well field vs year from 2008 to 2021 (BWB data)

*Figure deleted for data protection reasons*

Figure 18: Observed chloride concentration in K-well field vs year per abstraction (BWB data)

Table 6: Chlorid Analysen vom BWB Hydrochemie ab 2020 Langer See

<b>Probenahme Datum</b>	<b>Chlorid (mg/l)</b>
08.01.2020	48
04.02.2020	46
02.03.2020	44
03.06.2020	52
27.07.2020	54
10.08.2020	55
08.09.2020	57
03.11.2020	49
01.12.2020	47
05.01.2021	49
07.04.2021	47
04.05.2021	49
01.06.2021	49
27.07.2021	51
24.08.2021	50
05.10.2021	47
02.11.2021	49

Table 7: Well field K profiles 1983

*Table deleted for data protection reasons*

*Figure deleted for data protection reasons*

Figure 19: Profilschnitt K-Galerie Nord- Süd von Asbrand-Ing

*Figure deleted for data protection reasons*

Figure 20: Profilschnitt K-galerie Ost-West von Asbrand-Ing

**Annex 2: Supplementary results for model scenarios**

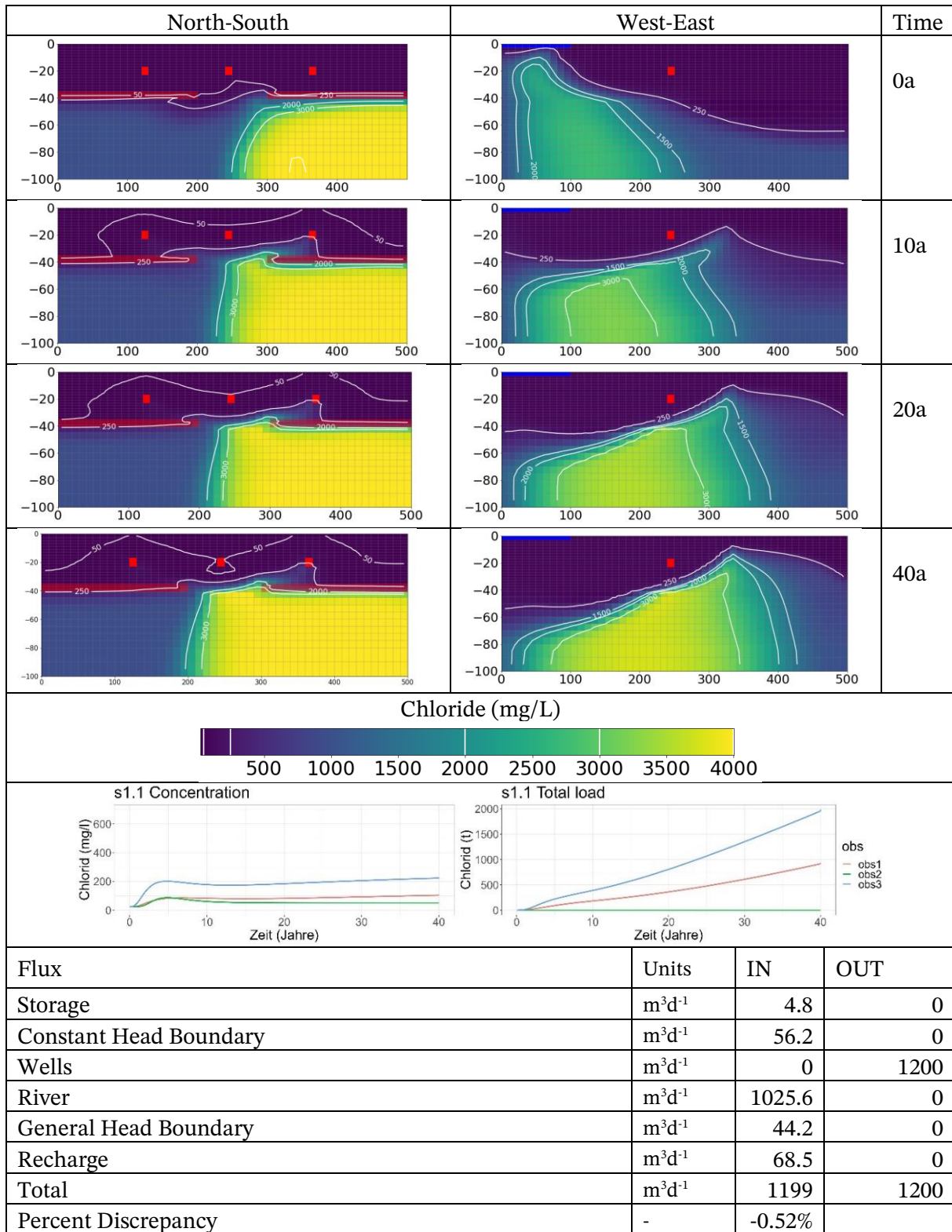


Figure 21: Cross sections, breakthrough curve, and water budget for scenario S1.1;  $Q_2 = 0 \text{ m}^3\text{d}^{-1}$

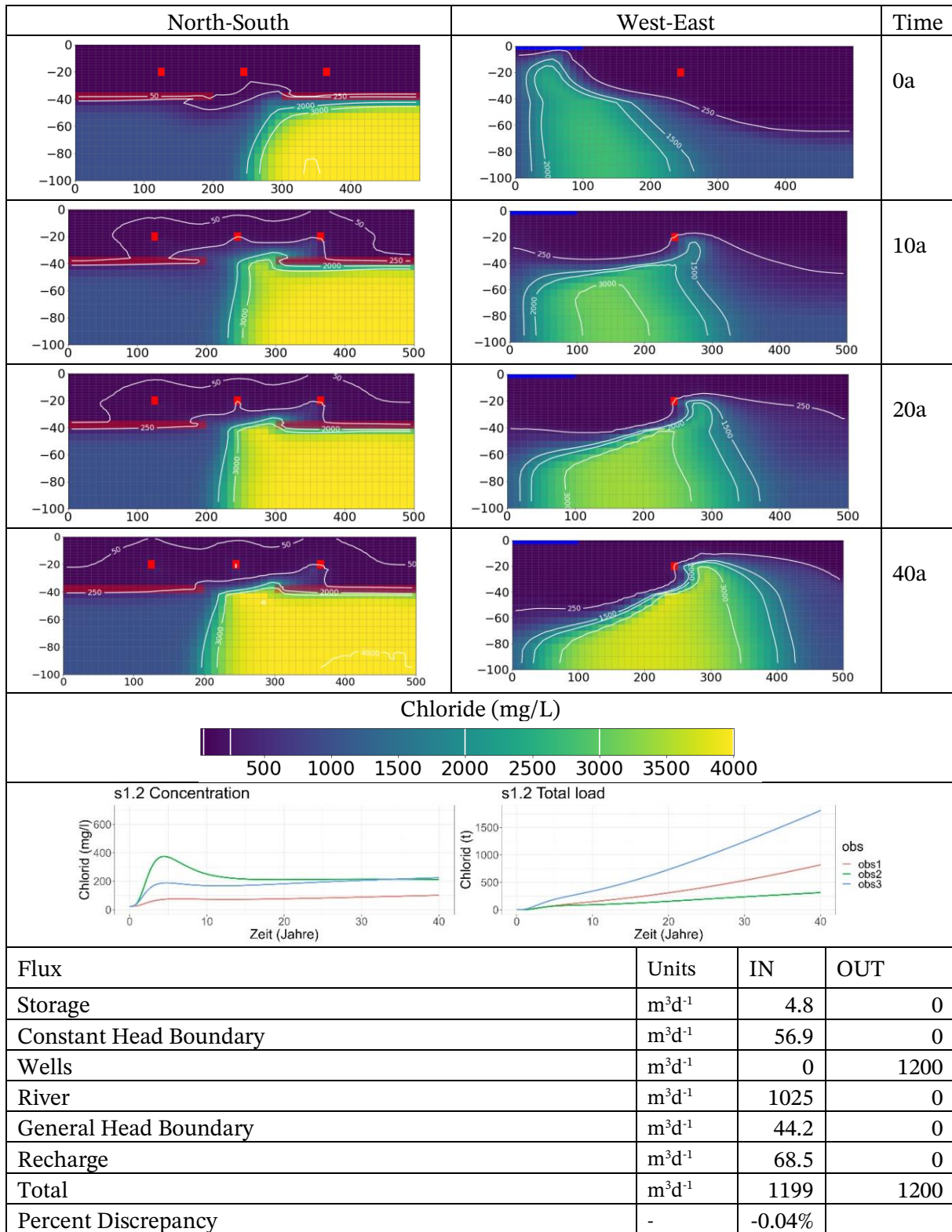


Figure 22: Cross sections, breakthrough curve, and water budget for scenario S1.2;  $Q_2 = 100 m^3d^{-1}$

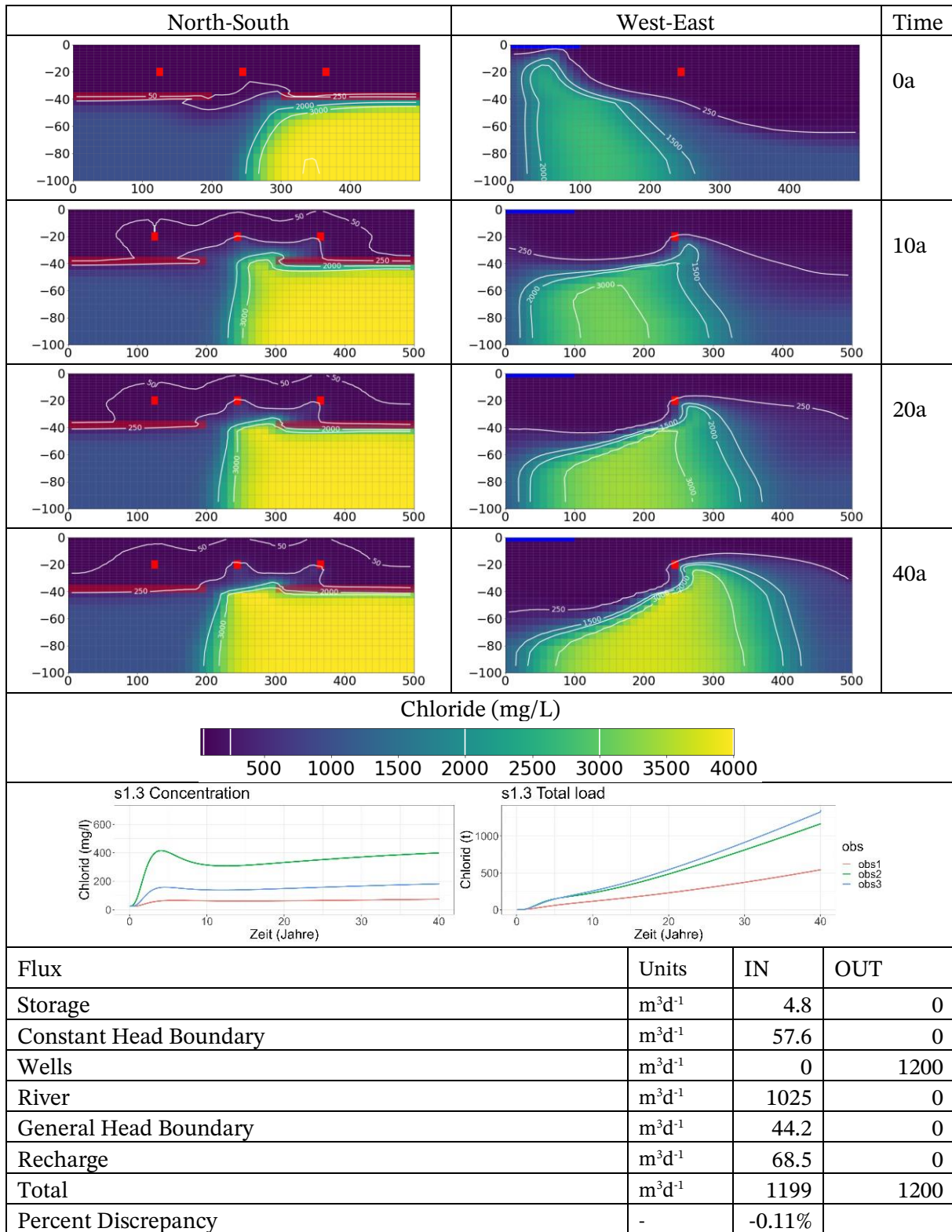


Figure 23: Cross sections, breakthrough curve, and water budget for scenario S1.3;  $Q_2 = 200 m^3d^{-1}$

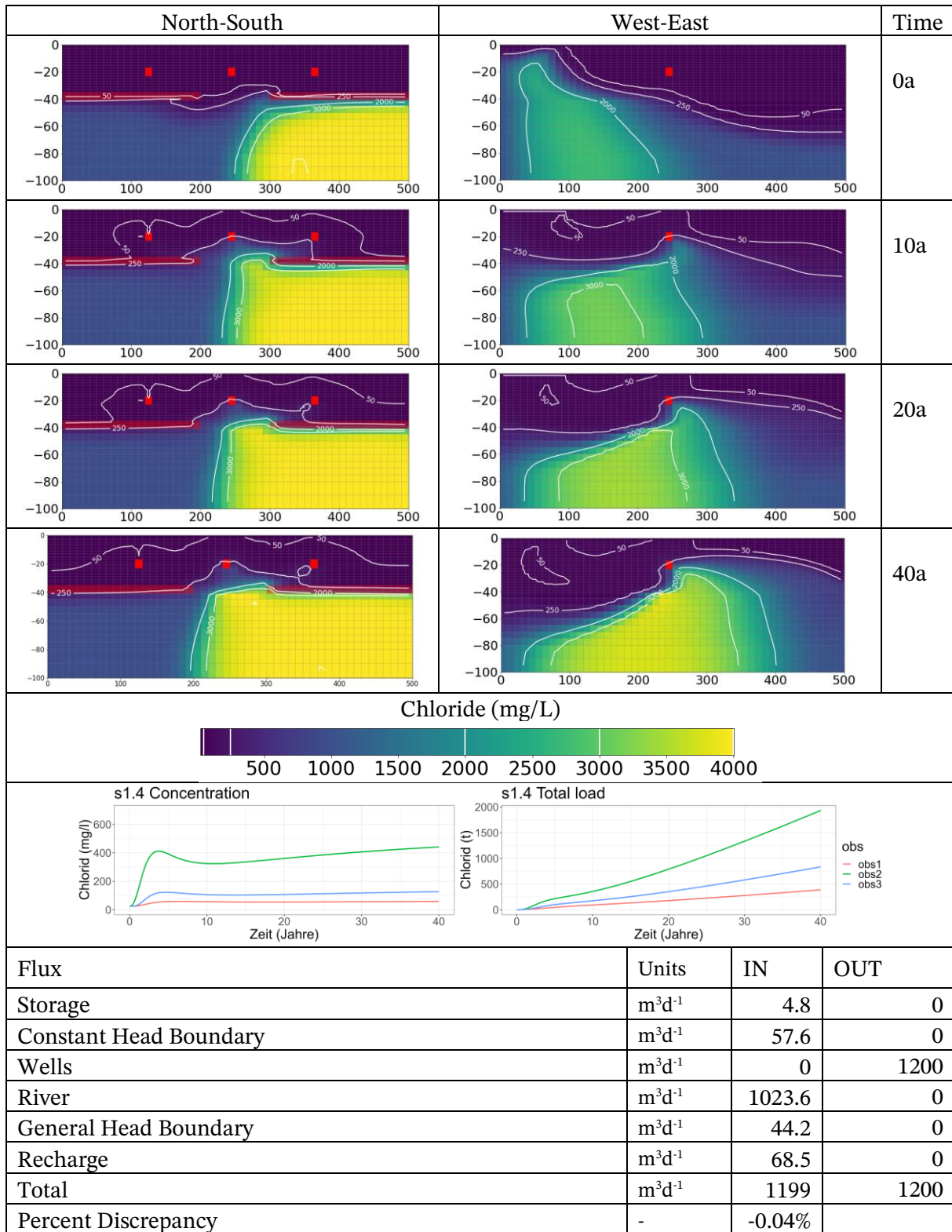


Figure 24: Cross sections, breakthrough curve, and water budget for scenario S1.4;  $Q_2=300 \text{ m}^3\text{d}^{-1}$

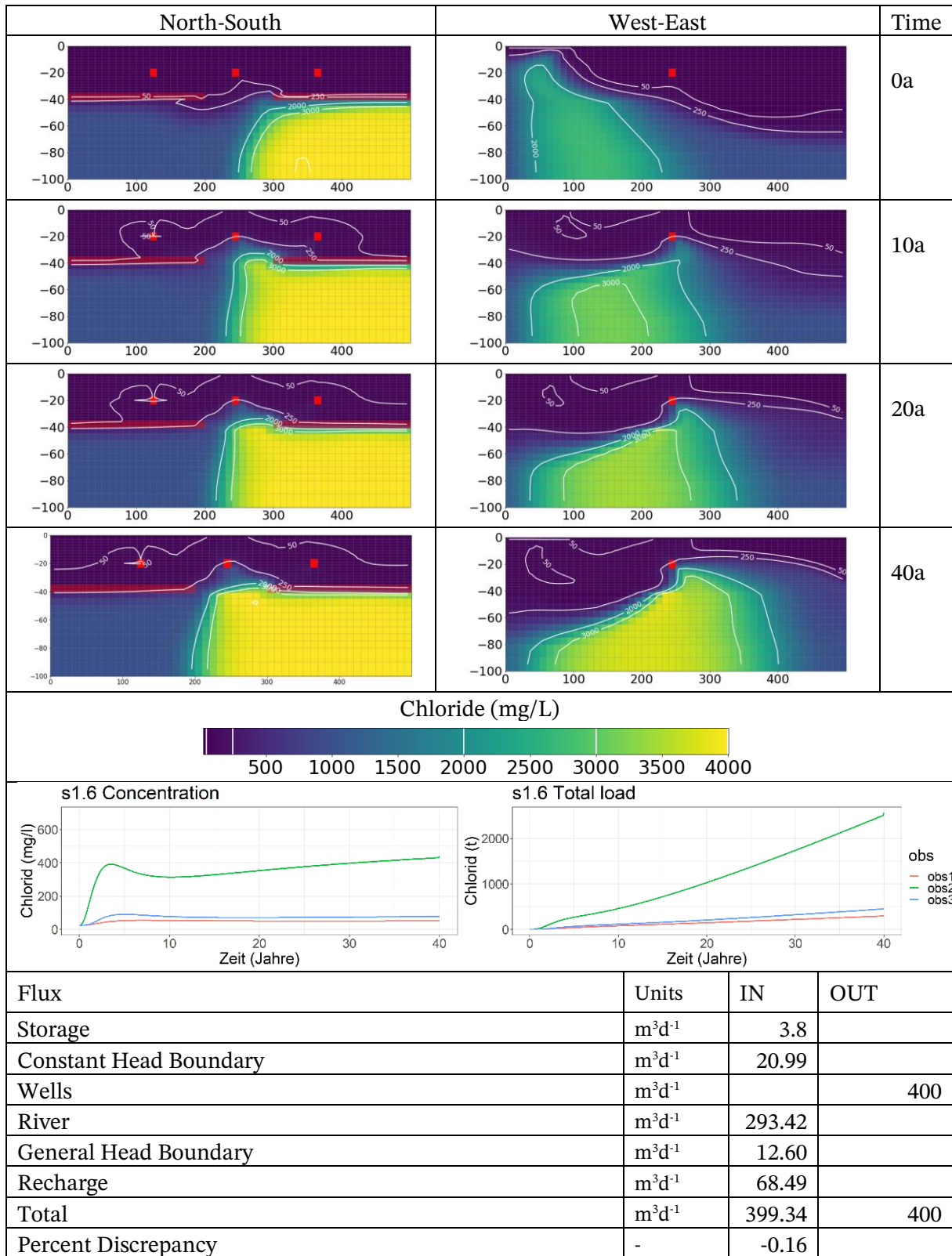


Figure 25: Cross sections, breakthrough curve, and water budget for scenario S1.6;  $Q_2=400 m^3d^{-1}$

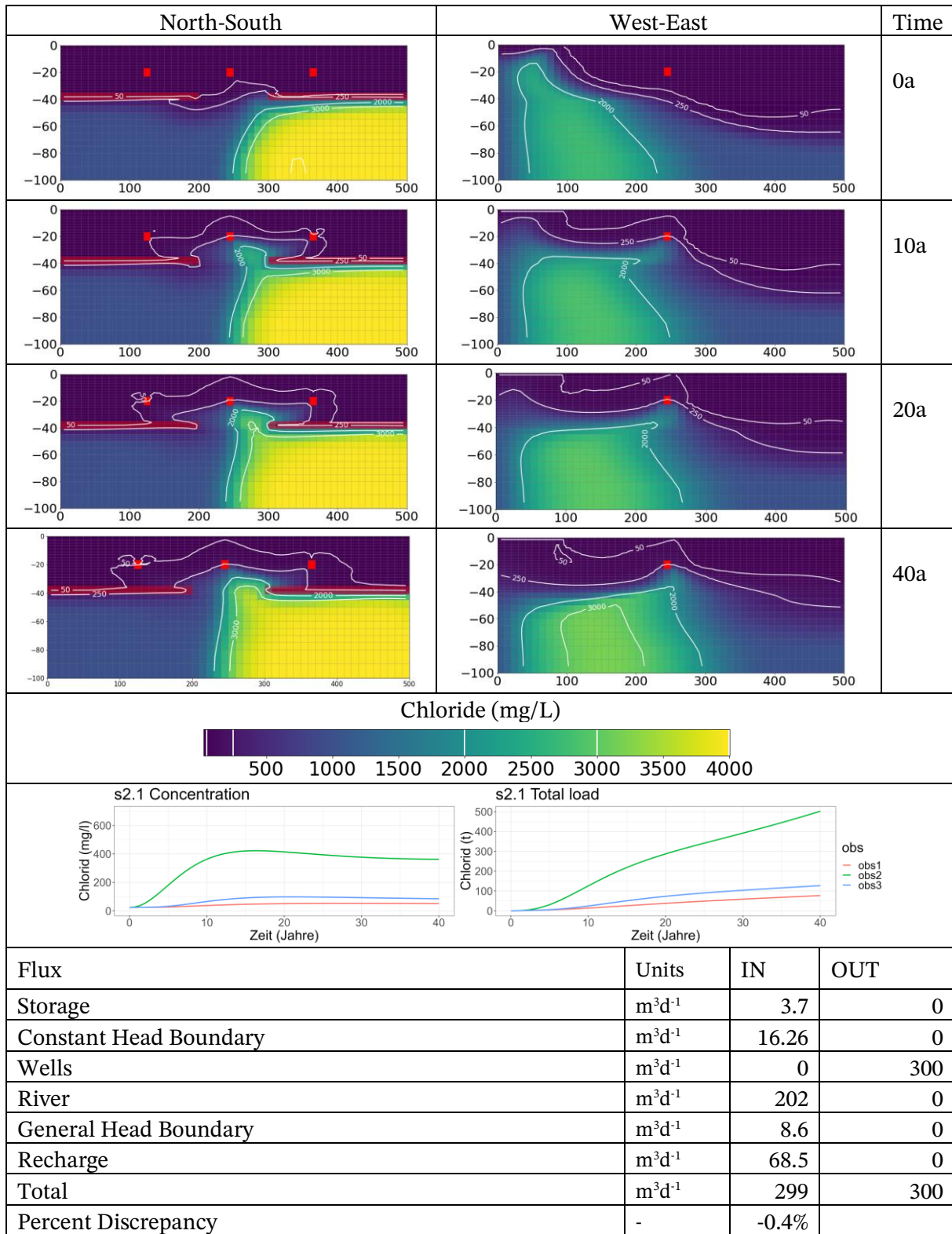


Figure 26: Cross sections, breakthrough curve, and water budget for scenario S2.1;  $Q_{\text{TOT}} = 300 \text{ m}^3\text{d}^{-1}$

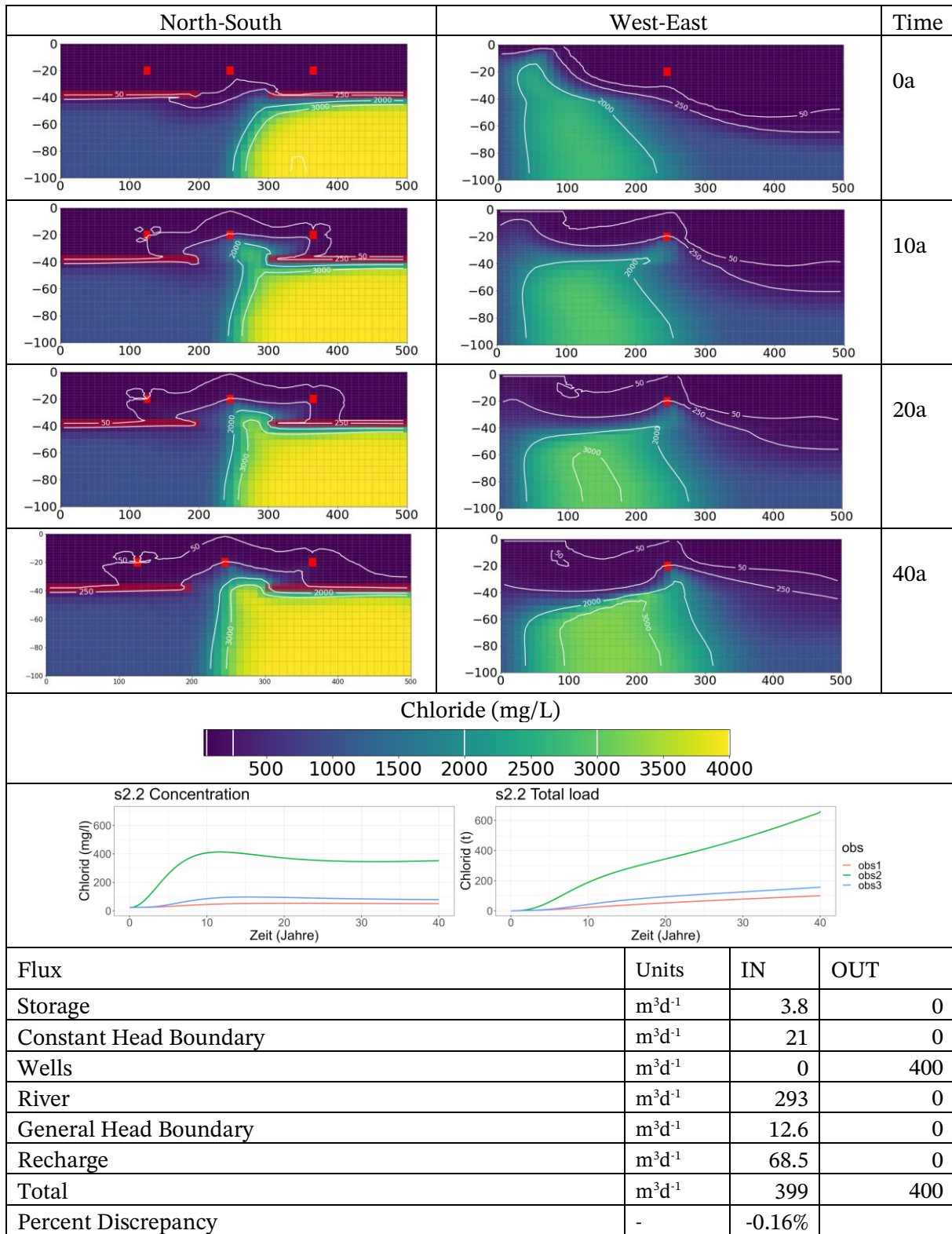


Figure 27: Cross sections, breakthrough curve, and water budget for scenario S2.2;  $Q_{\text{TOT}} = 400 \text{ m}^3\text{d}^{-1}$

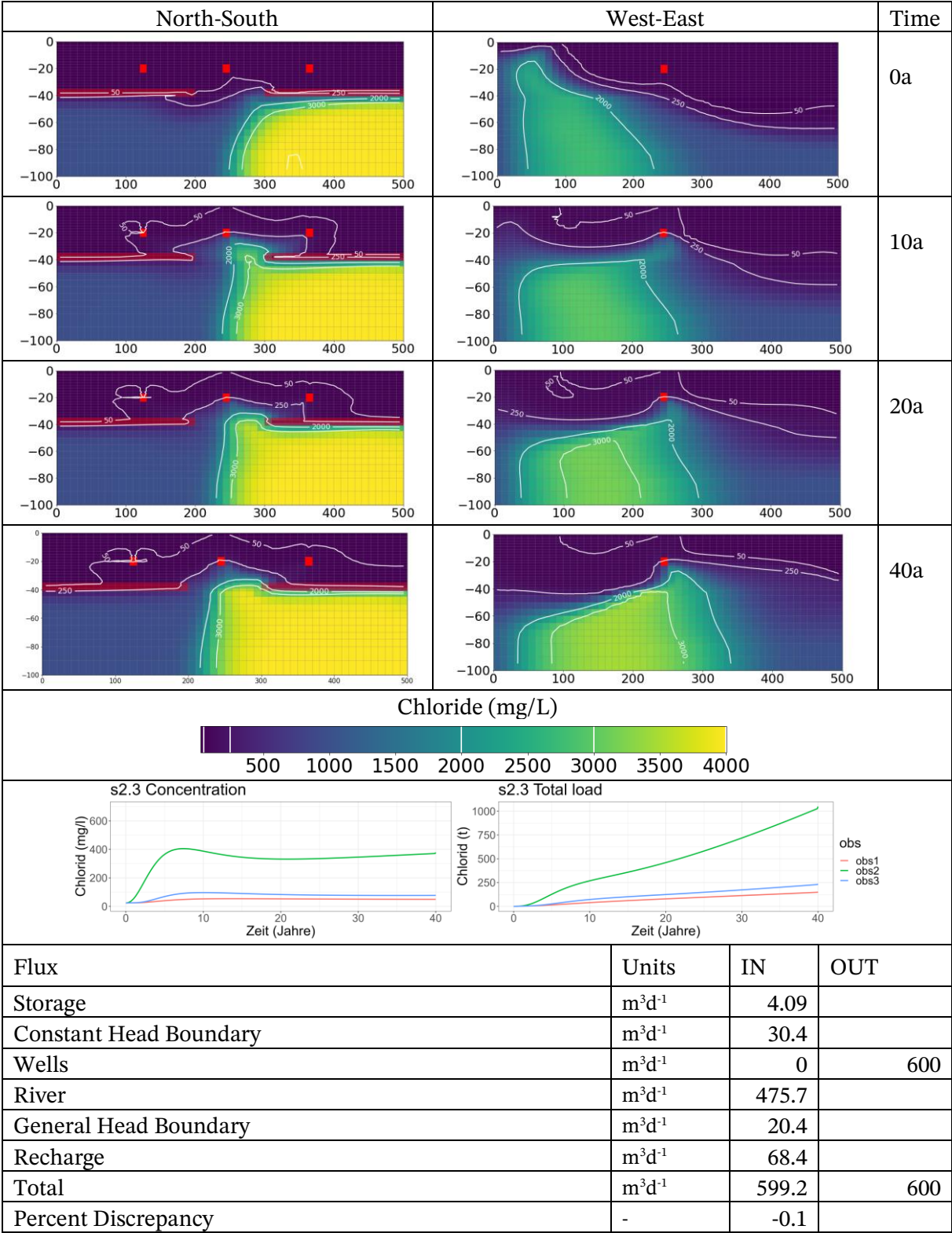


Figure 28: Cross sections, breakthrough curve, and water budget for scenario S2.3;  $Q_{TOT} = 600 m^3d^{-1}$

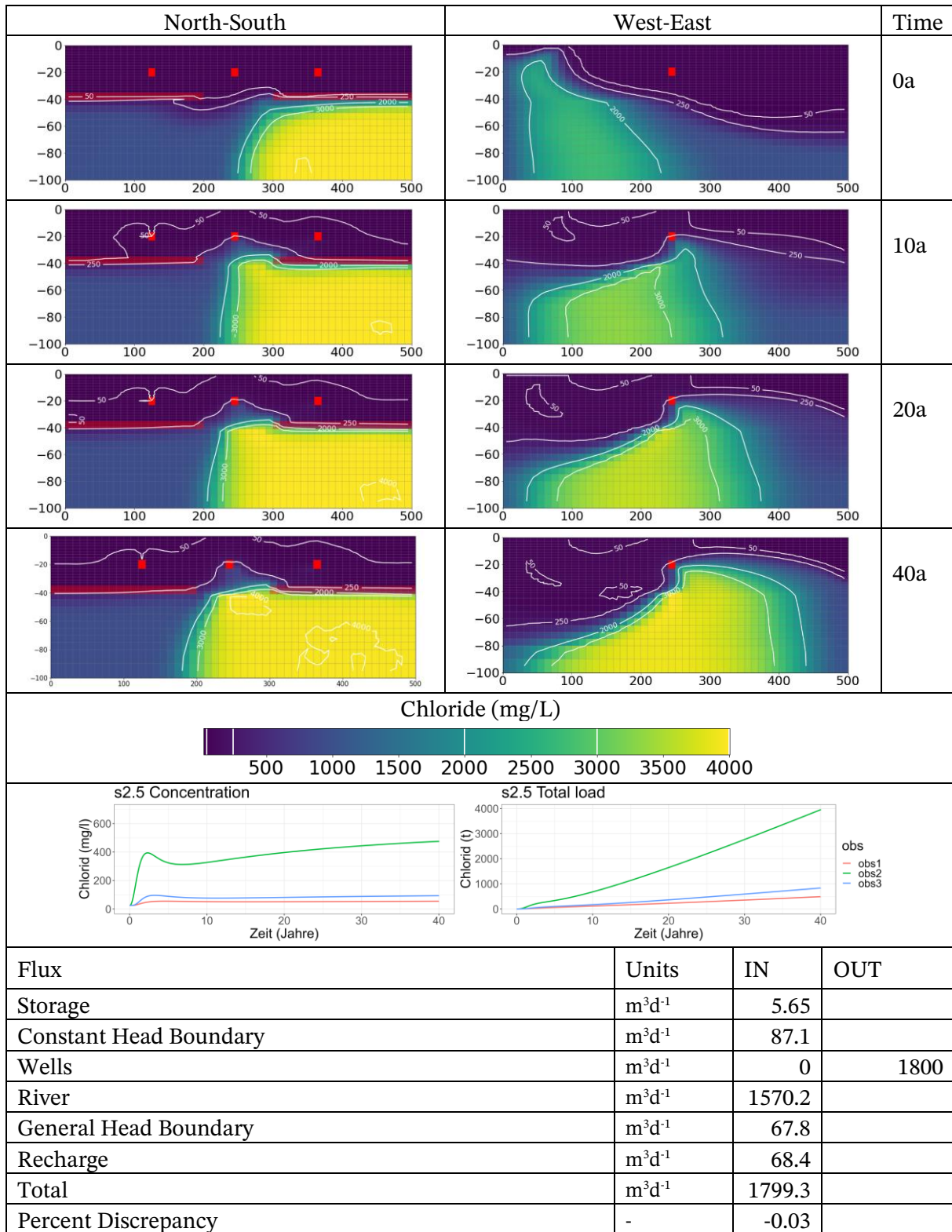


Figure 29: Cross sections, breakthrough curve, and water budget for scenario S2.5;  $Q_{TOT} = 1800 m^3d^{-1}$

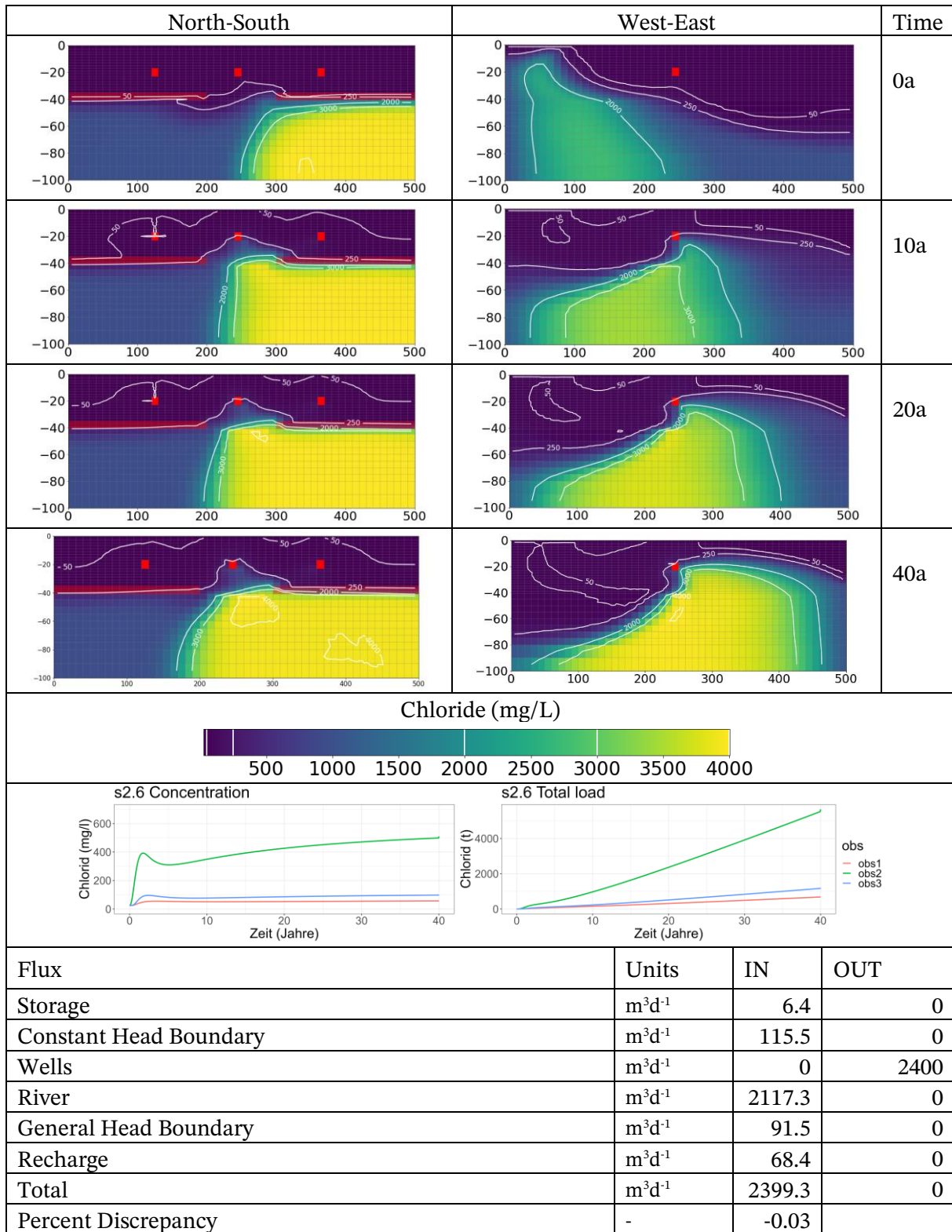


Figure 30: Cross sections, breakthrough curve, and water budget for scenario S2.6;  $Q_{TOT} = 2400 m^3d^{-1}$

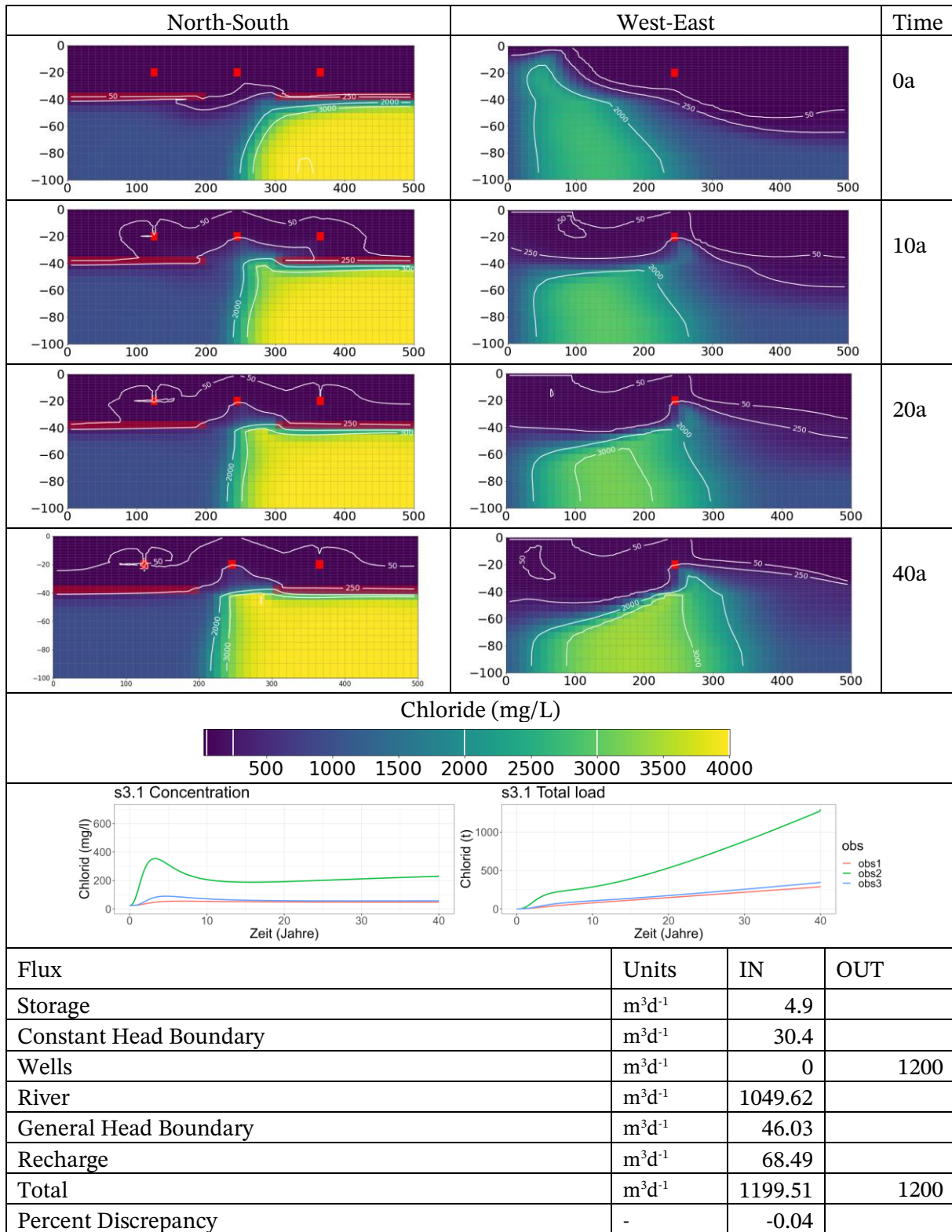


Figure 31: Cross sections, breakthrough curve, and water budget for scenario S3.1

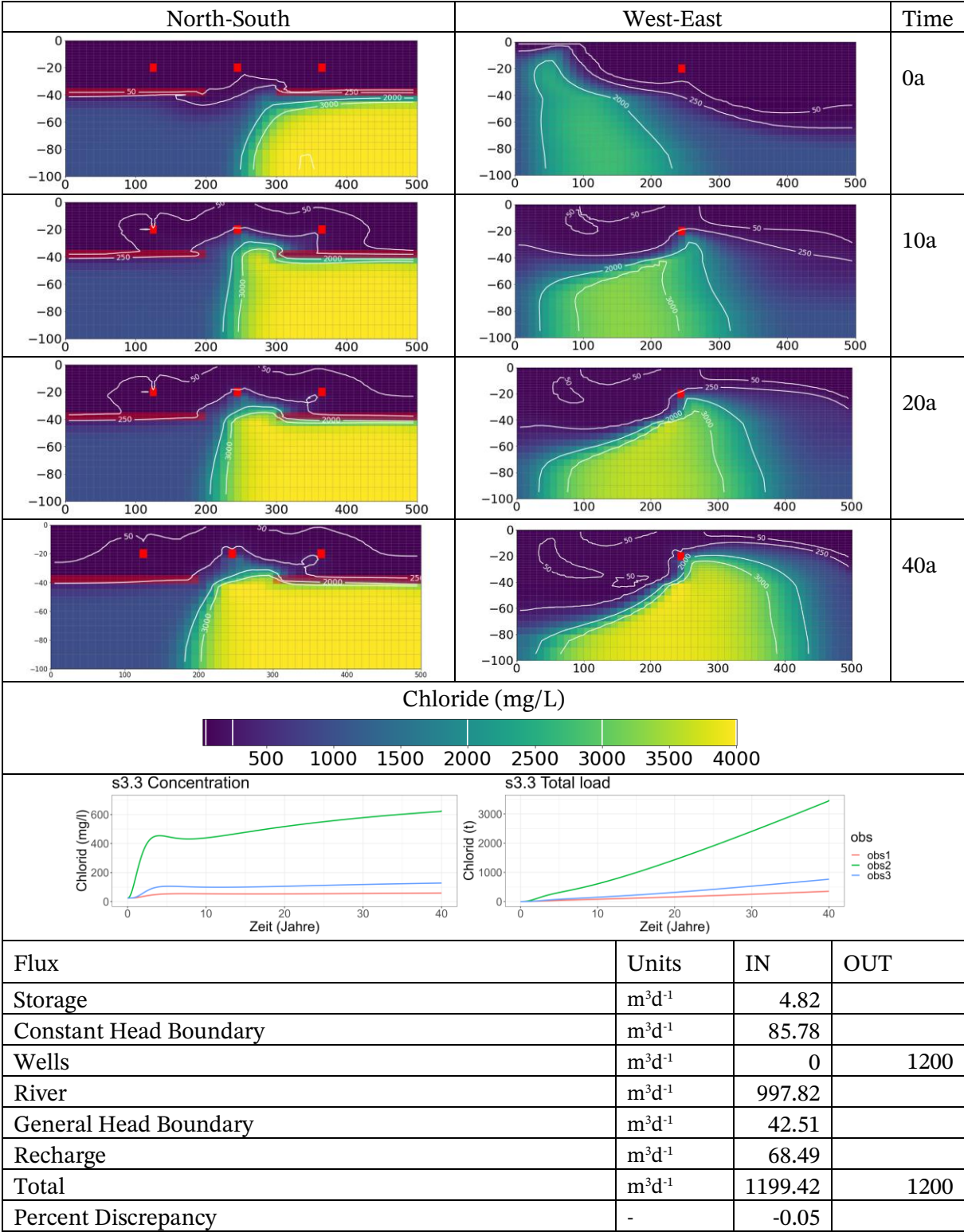


Figure 32: Cross sections, breakthrough curve, and water budget for scenario S3.3

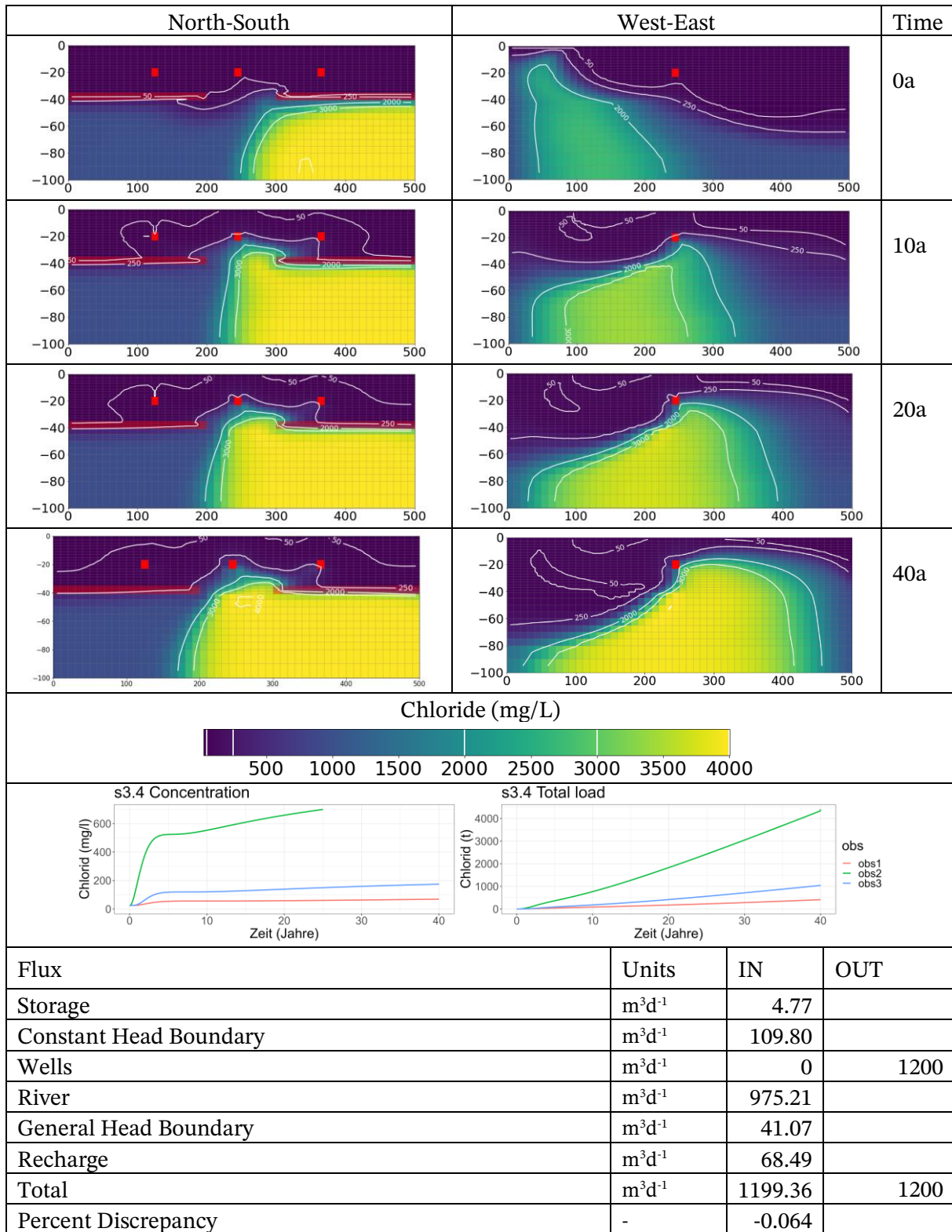


Figure 33: Cross sections, breakthrough curve, and water budget for scenario S3.4

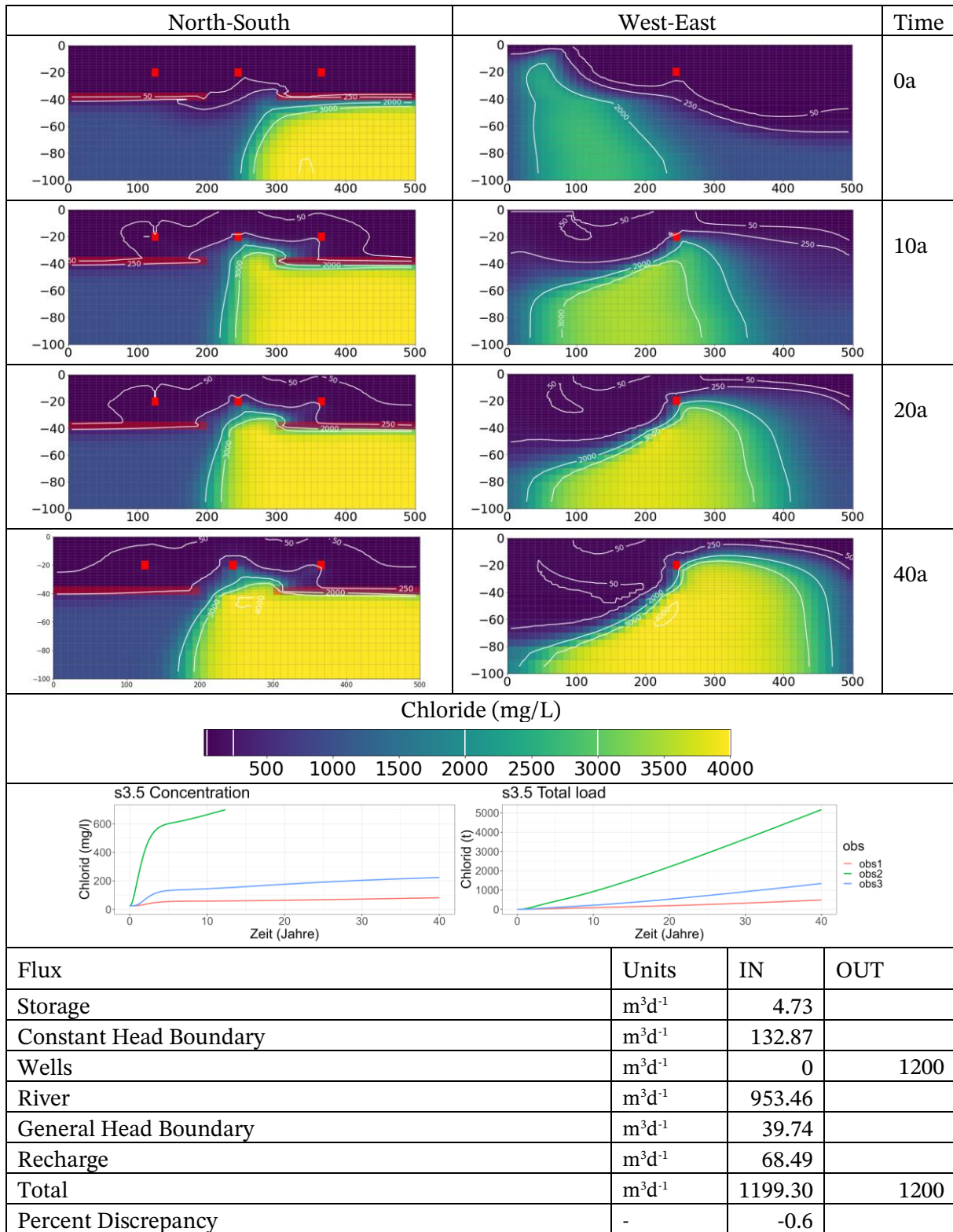


Figure 34: Cross sections, breakthrough curve, and water budget for scenario S3.5

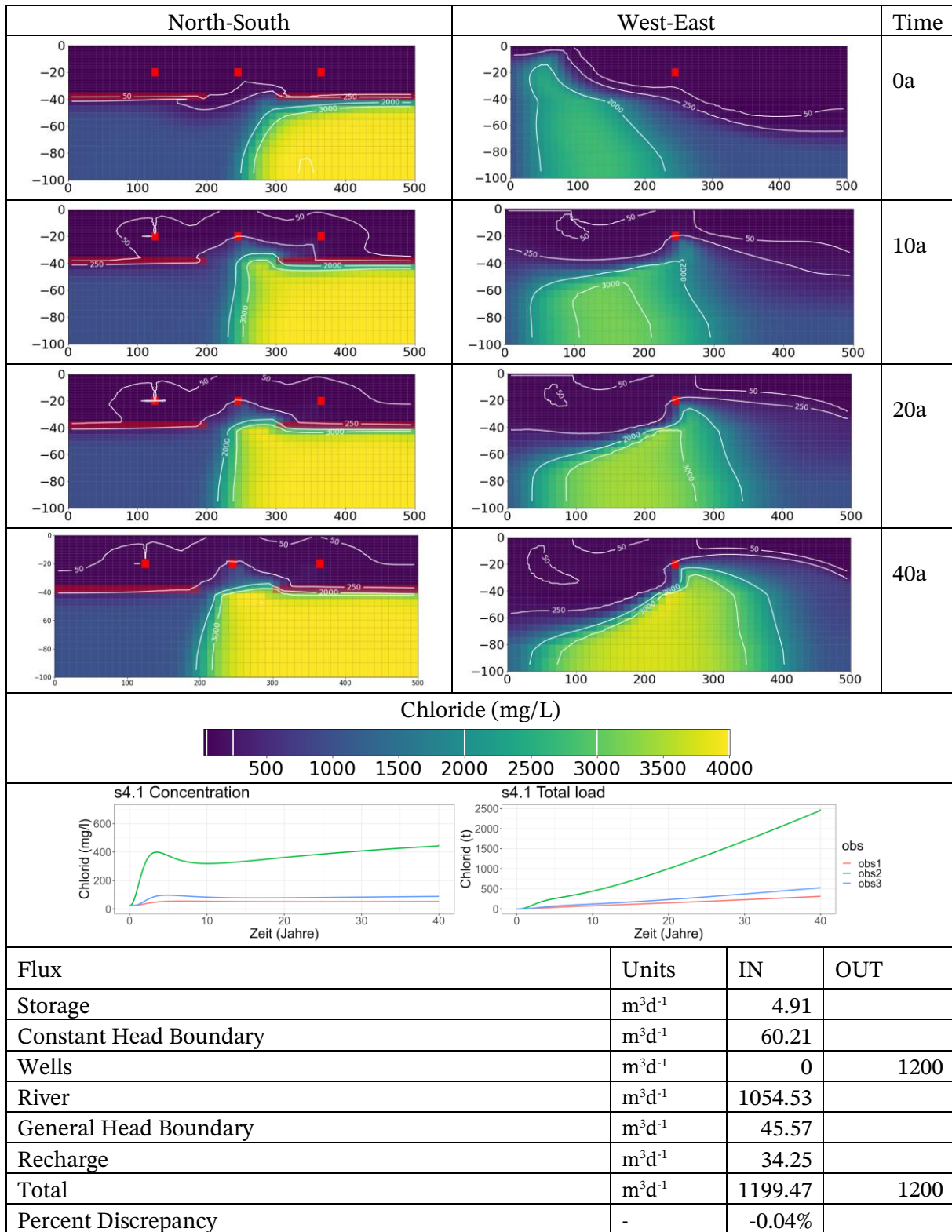


Figure 35: Cross sections, breakthrough curve, and water budget for scenario S4.1

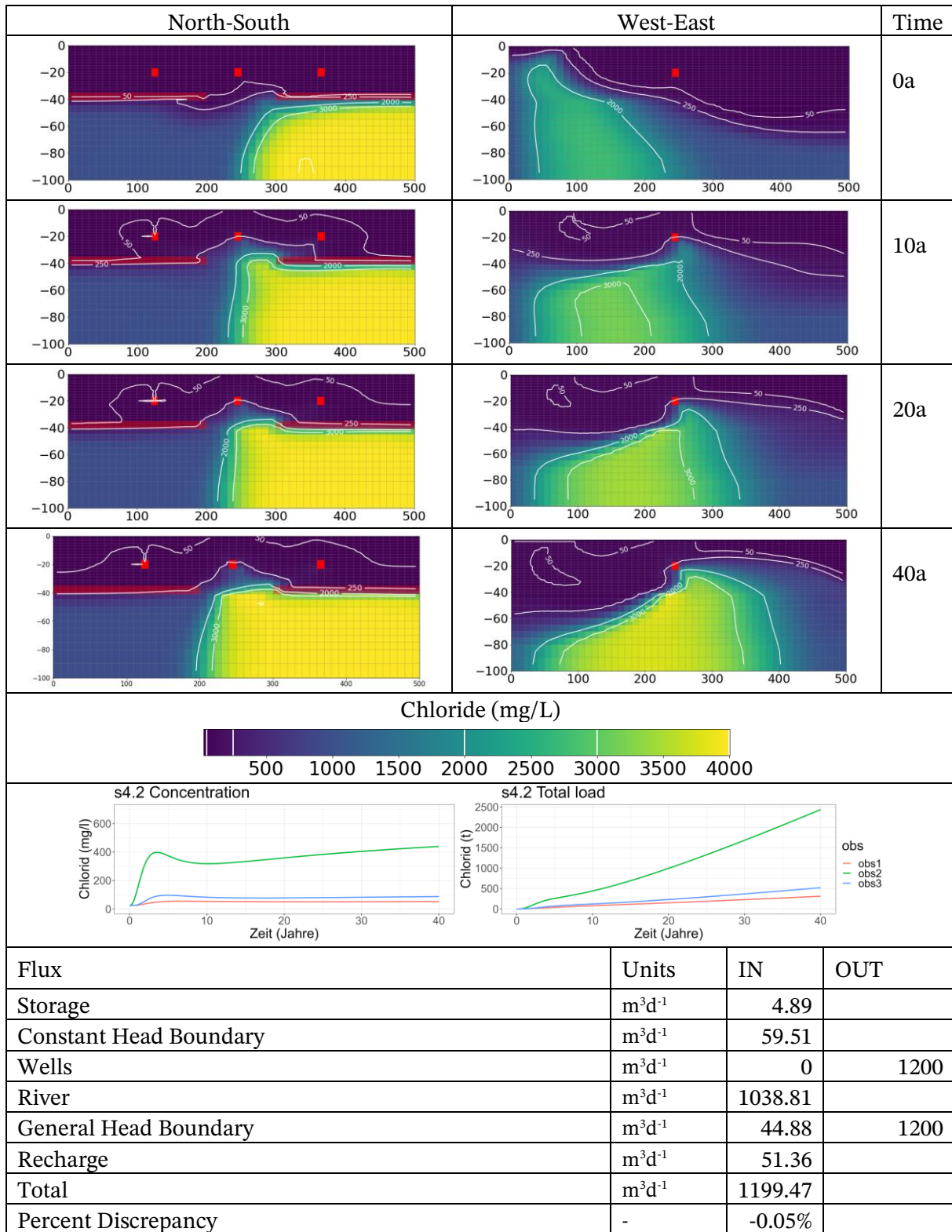


Figure 36: Cross sections, breakthrough curve, and water budget for scenario S4.2

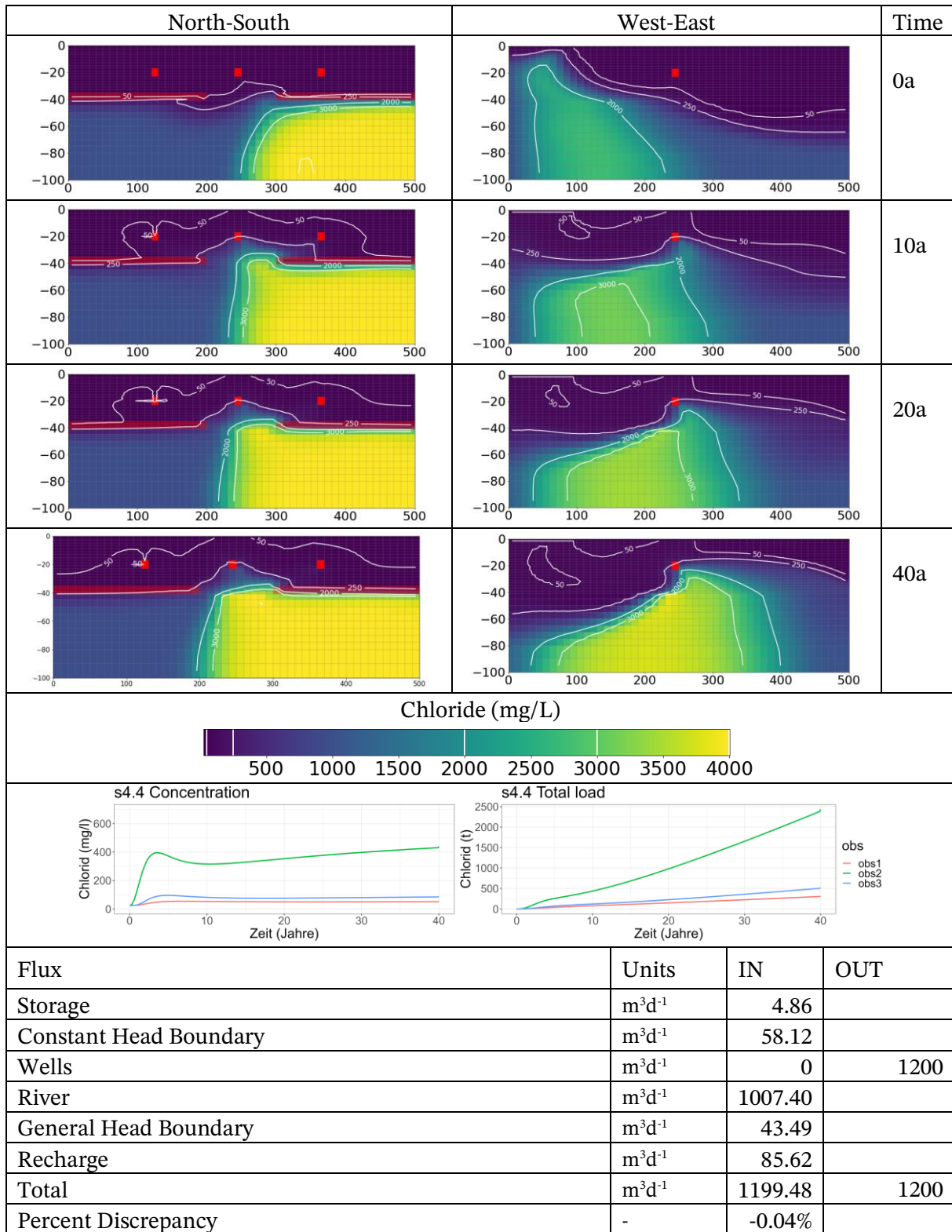


Figure 37: Cross sections, breakthrough curve, and water budget for scenario S4.4

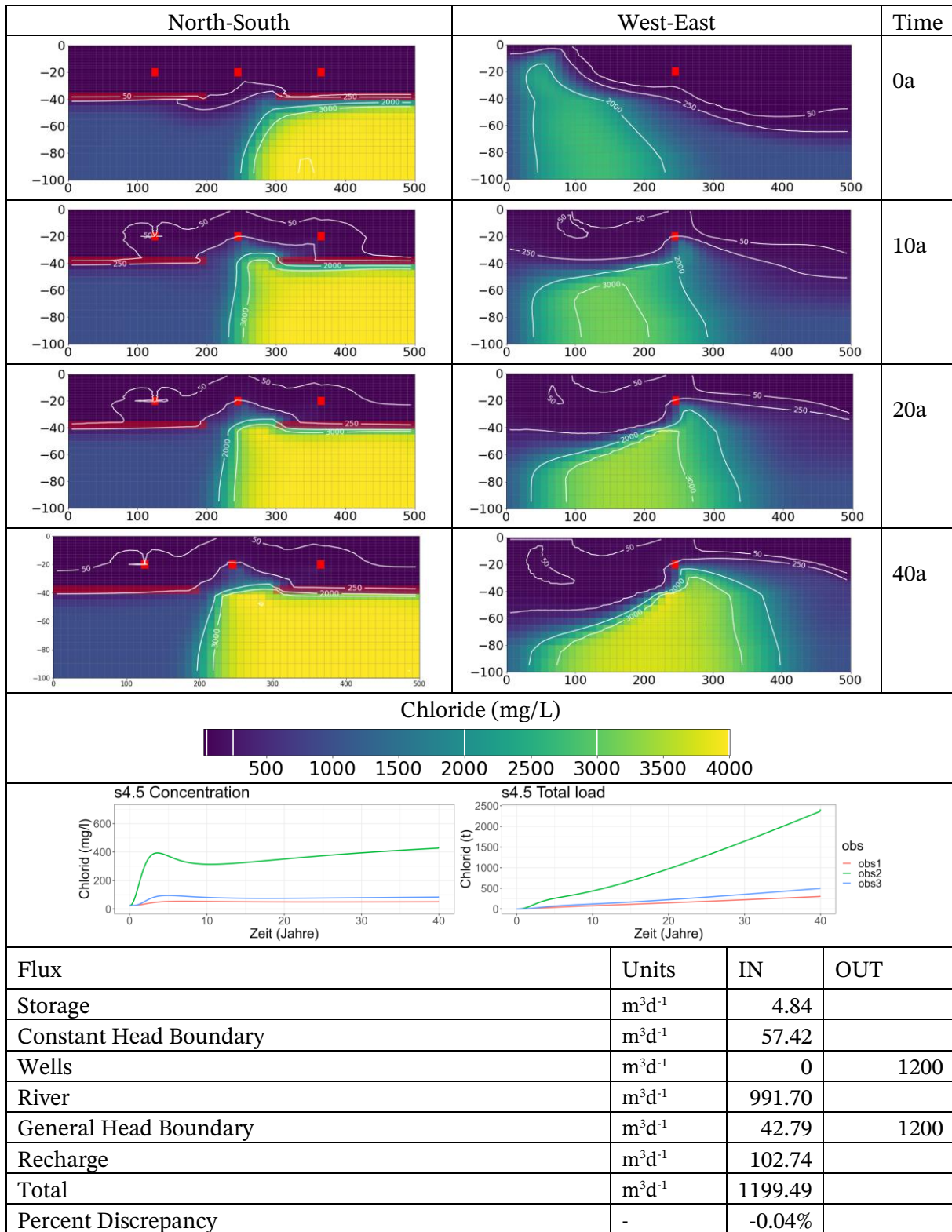


Figure 38: Cross sections, breakthrough curve, and water budget for scenario S4.5

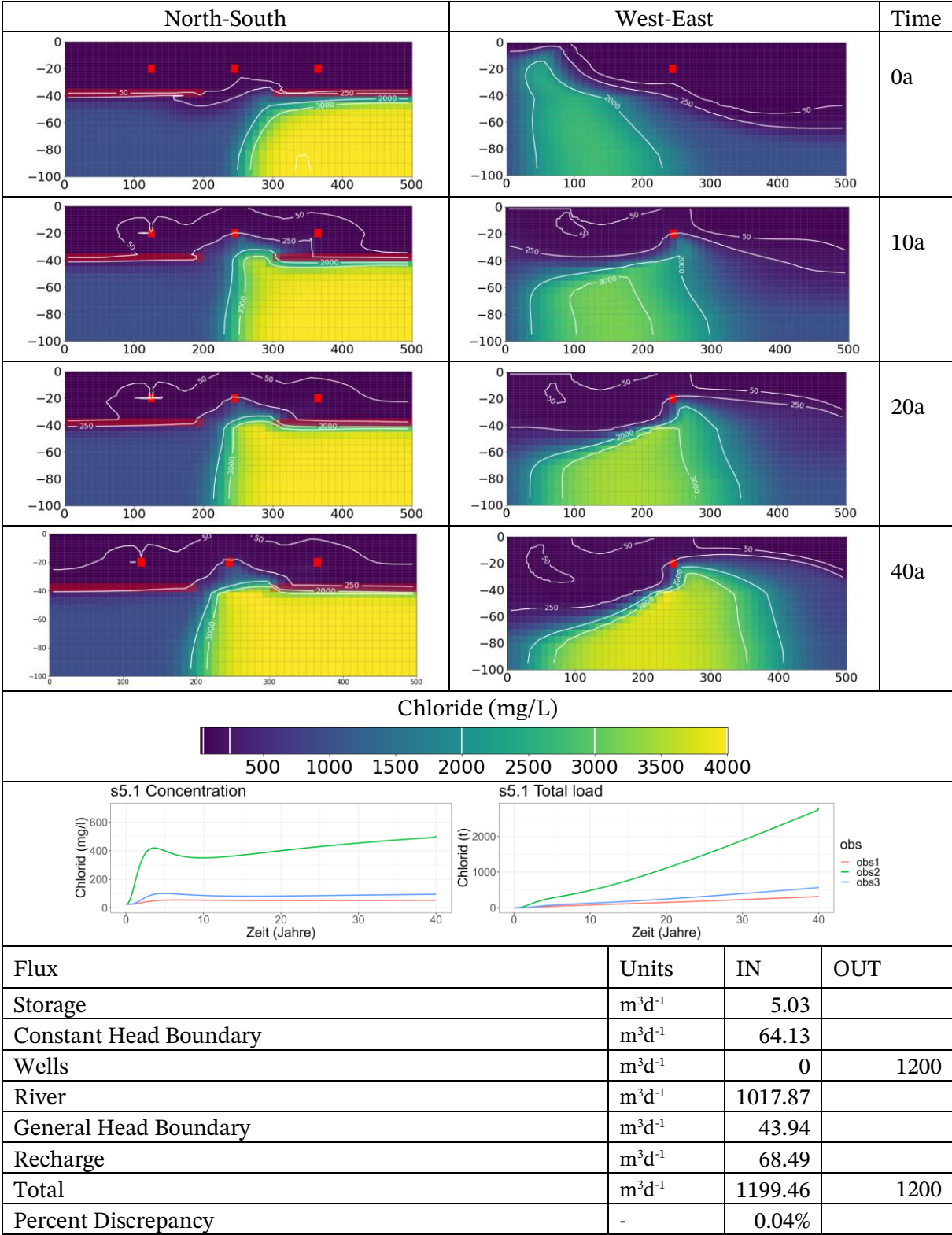


Figure 39: Cross sections, breakthrough curve, and water budget for scenario S5.1

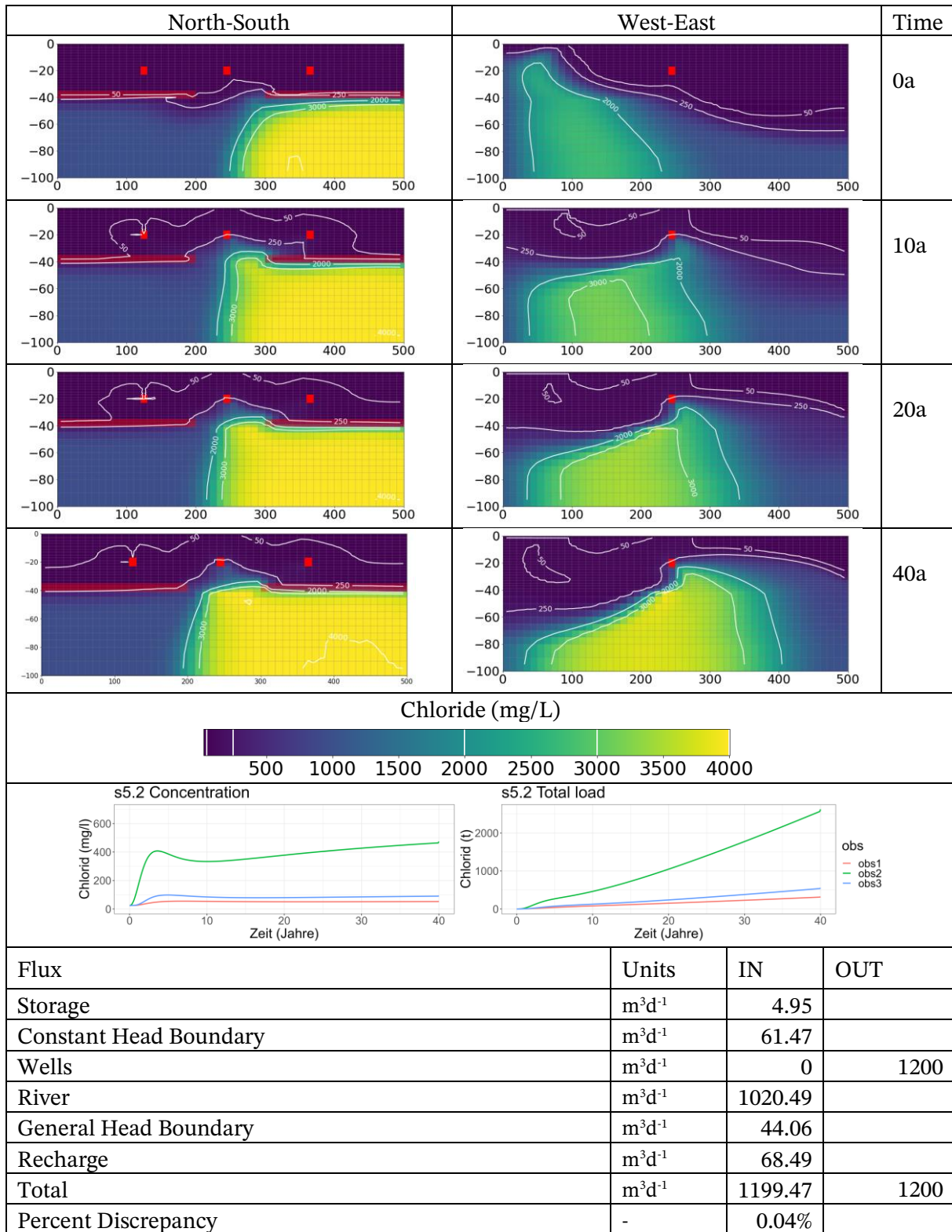


Figure 40: Cross sections, breakthrough curve, and water budget for scenario S5.2

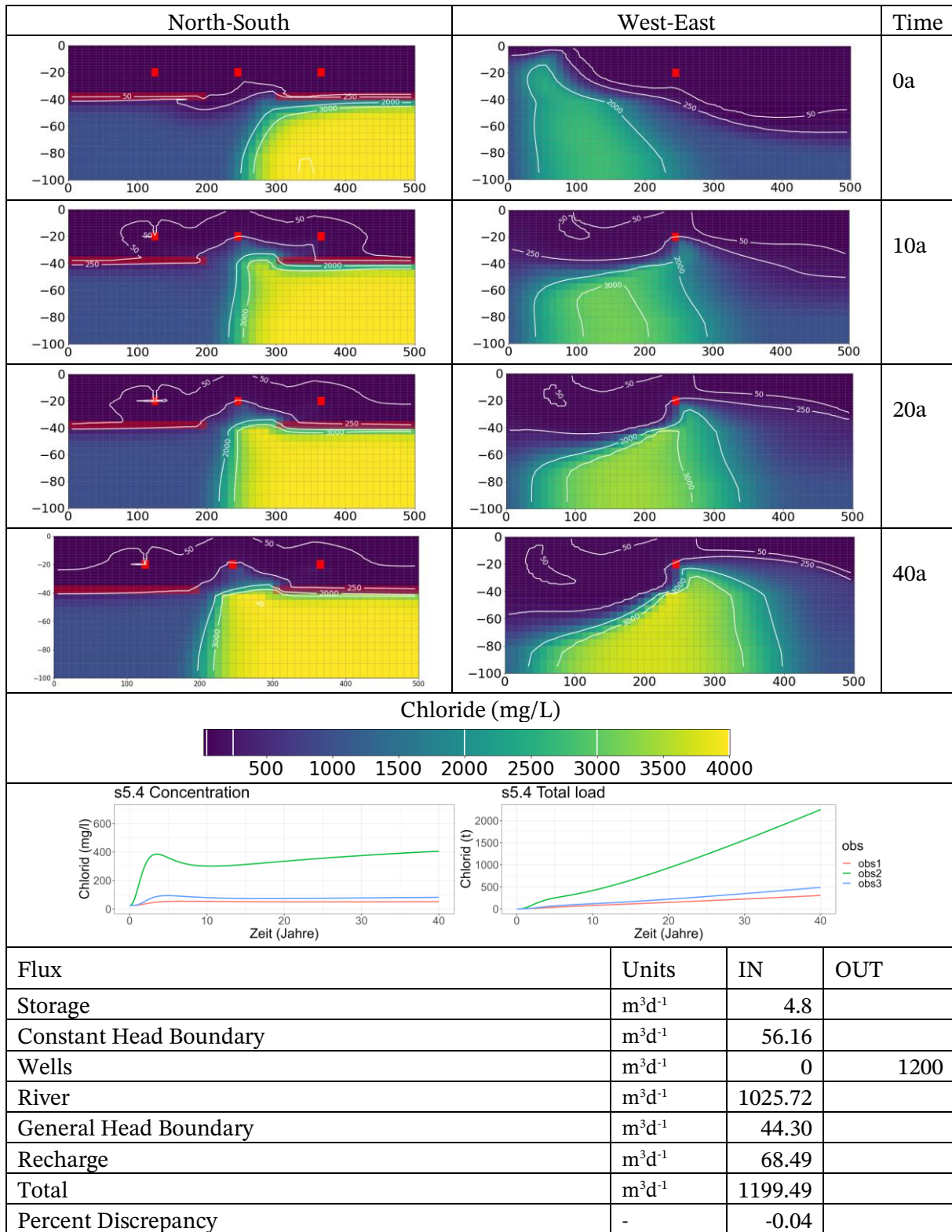


Figure 41: Cross sections, breakthrough curve, and water budget for scenario S5.4

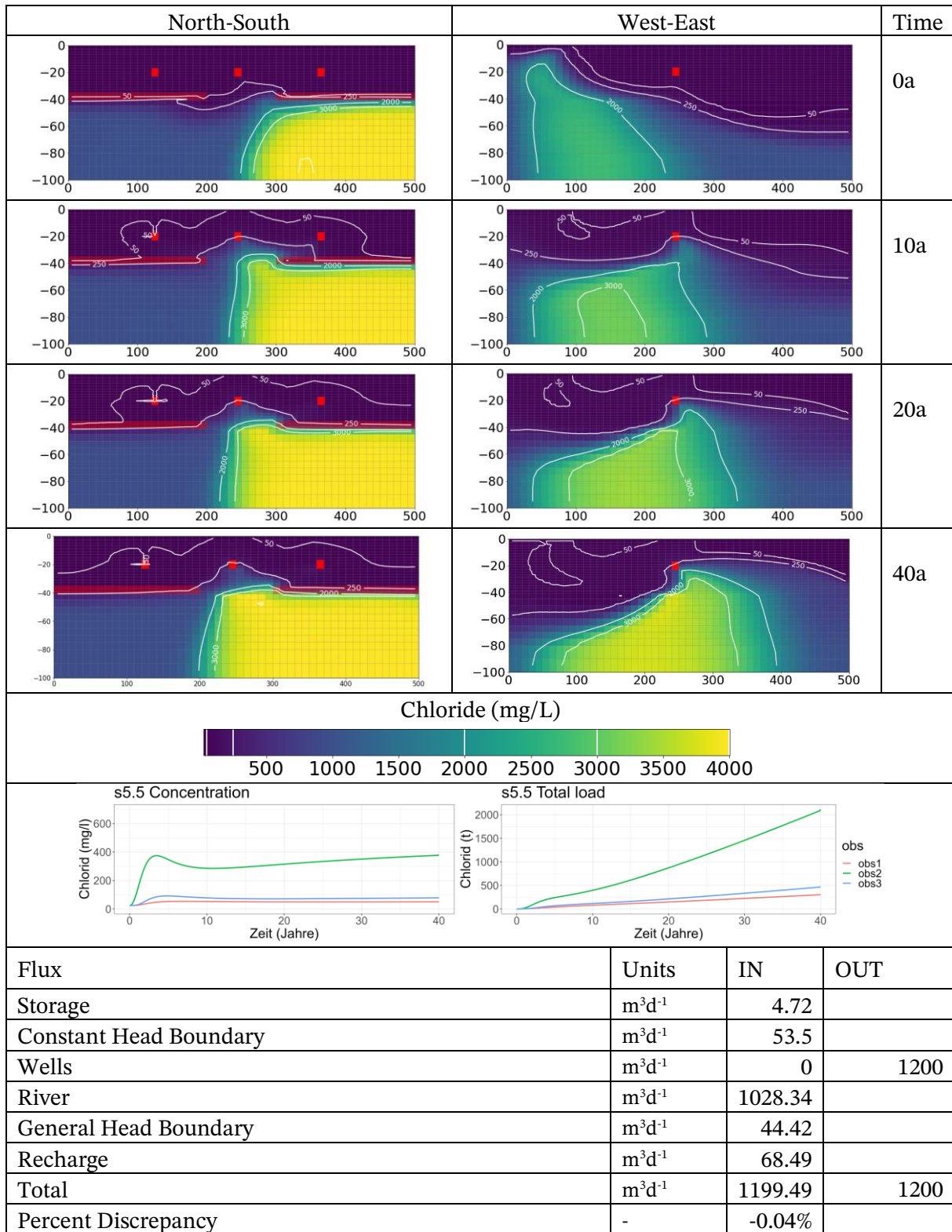


Figure 42: Cross sections, breakthrough curve, and water budget for scenario S5.5

## **KWB      Kompetenzzentrum      Wasser      Berlin** **gemeinnützige GmbH**

Grunewaldstr.61-62, D-10825 Berlin

[www.kompetenz-wasser.de](http://www.kompetenz-wasser.de)

**Follow us:**

LinkedIn: [Kompetenzzentrum Wasser Berlin](#)

Twitter: [@kompetenzwasser](#)